UNIVERSITÉ DU QUÉBEC À RIMOUSKI

Nature et origine des sédiments de surface de l'estuaire du Saint-Laurent

mémoire présenté

dans le cadre du programme de maîtrise en océanographie

en vue de l'obtention du grade de maître ès science

PAR

© MATTHIEU JAEGLE

Mars 2015

Composition du jury :

Urs Neumeier, président du jury, UQAR-ISMER

Guillaume St-Onge, directeur de recherche, UQAR-ISMER

Jean-Carlos Montero-Serrano, codirecteur de recherche, UQAR-ISMER

Patrick, Lajeunesse, codirecteur de recherche, U.Laval

John T. Andrews, examinateur externe, INSTAAR, Université du Colorado

Dépôt initial le 26 septembre 2014 Dépôt final le 25 mars 2015

Je ne suis pour toi qu'un renard semblable à cent mille renards. Mais, si tu m'apprivoises, nous aurons besoin l'un de l'autre. Tu seras pour moi unique au monde. Je serai pour toi unique au monde...

Le petit prince - Antoine de Saint-Exupéry

REMERCIEMENTS

Je tiens en premier lieu à remercier Guillaume St-Onge pour la qualité son encadrement, sa disponibilité, ses nombreux conseils et opportunités offertes au cours de ma maitrise. Mais surtout, je tiens à souligner sa capacité à transmettre sa passion pour la sédimentologie, véritable clé de voute pour la réussite d'une maitrise. Je souhaite également remercier chaleureusement Jean-Carlos Montero-Serrano pour sa gentillesse exemplaire, pour avoir rejoint l'équipe en cours de route et pour avoir donner un nouvel élan au projet. Mes remerciements vont également à Patrick Lajeunesse pour son encadrement et pour l'accessibilité au N/R Louis-Edmond-Hamelin. J'aimerais également apporter toute ma gratitude à Urs Neumeier pour l'évaluation de mon mémoire et également pour les nombreuses discussions scientifiques partagées lors de cours ainsi que pour la confiance accordée lors de la mission stage en 2013. Je remercie aussi le membre externe de mon jury d'évaluation, professeur John T. Andrews.

Je souhaite également remercier l'ensemble des personnes ayant rendu mon projet et mes travaux de terrain possibles. Merci à Adrien Bénard, capitaine du Louis-Edmond-Hamelin et merci à l'ensemble de l'équipage du N/R Coriolis II. Merci à Alexandre Normandeau, Gabriel Joyal, Marie-Pier St-Onge et Jacques Labrie pour votre aide sur le terrain ou en laboratoire.

Merci à l'ensemble du laboratoire de géologie et autres compères de l'ISMER, Quentin, Elissa, Pierre-Arnaud, Audrey, Julie, Kevin, Gab, Mélany, Étienne, Colette pour vos précieux conseils, vos sourires et vous encouragements. Merci pour les bières et les cafés partagés quand la motivation n'était plus à son maximum. Je souhaite également remercier l'ensemble des habitants de la maison au toit rouge, Denys, Julien, Yann,

Vincent, Leuth, Flora pour m'avoir supporté au cours de ma maitrise, pour avoir rendu ma vie extrascolaire si aisée avec une ambiance merveilleuse.

Mes derniers remerciements s'adressent à mes parents, à ma sœur et ma copine, merci d'avoir toujours cru en moi et d'avoir écouté mes interminables questionnements « existentielles » sur le sable.

RÉSUMÉ

La composition minéralogique, les propriétés magnétiques et la distribution granulométrique des sédiments de surface de l'estuaire du Saint-Laurent ont été étudiées afin d'associer la nature des sédiments marins avec les caractéristiques géologiques des principales rivières adjacentes. La comparaison de ces propriétés et l'utilisation de l'analyse en composantes principales ont permis de discriminer deux sources distinctes : la Côte-Nord et la Rive-Sud. La Côte-Nord se caractérise par une forte teneur en feldspath et une intensité magnétique élevée, alors que la Rive-Sud présente des concentrations plus élevées en phyllosilicates et en quartz, ainsi qu'une intensité magnétique plus faible. La discrimination de ces deux sources reflète les différentes lithologies du substratum rocheux respectif : (1) les roches métamorphiques et ignées du Bouclier canadien sur la Côte-Nord, et (2) les roches sédimentaires appartenant aux Appalaches sur la Rive-Sud. Les sédiments marins d'eau peu profonde échantillonnés le long de la Côte-Nord présentent un comportement magnétique et une composition minéralogique similaire aux roches terrestres adjacentes. Des variations sont par contre observées dans le milieu marin profond (200-300 m, chenal Laurentien) avec une diminution en quartz et plagioclases et une augmentation en mica et en argile, ainsi qu'une diminution de la susceptibilité magnétique par rapport aux sédiments côtiers. Ces propriétés sont également associées à une diminution de la taille des grains, reflétant des conditions hydrodynamiques plus faibles dans le chenal Laurentien. D'autre part, les sédiments échantillonnés le long de la marge sud sont caractérisés par des propriétés inattendues, avec une composition minéralogique et des propriétés magnétiques plus proches des échantillons Côte-Nord que des échantillons de la Rive-Sud. Cette observation pourrait refléter des épisodes de transport glaciaire ou glaciel qui transporterait du matériel précambrien, tel que suggéré par différentes études antérieures soulignant la présence de blocs précambriens le long de la Rive-Sud. L'ensemble des résultats suggère que la Côte-Nord est la principale source d'alimentation en sédiments de l'estuaire et du golfe Saint-Laurent. Les variations de composition observées en milieu marin sont d'origines hydrodynamiques et la Rive-Sud ne contribue que faiblement dans le système. Ces observations sont en accord général avec les débits des rivières actuelles dans l'estuaire du Saint-Laurent, qui sont plus importants pour la Côte-Nord que pour la Rive-Sud.

Mots clés : sédiments, minéralogie, magnétisme, provenance, estuaire et golfe du Saint-Laurent

ABSTRACT

Mineralogical composition, magnetic properties, and grain size distribution of surface sediment samples from the St. Lawrence Estuary (eastern Canada) were investigated in order to constrain present-day sediment provenance in the marine environment in agreement with the geological characteristics of the main rivers. The intercomparison of these properties and the application of principal component analysis enabled the discrimination of two distinct sources. The North-Shore source is characterized by increased feldspar content and high values of the magnetic properties, whereas the South - Shore source exhibits higher concentrations of phyllosilicates and quartz, and weaker magnetic property values. The discrimination of these two sources reflects the different bedrock lithologies predominant in both shores: (1) the Grenvillian metamorphic and igneous rocks of the Canadian Shield on the North-Shore, and (2) the Early Palaeozoic sedimentary rocks belonging to the Appalachians Mountains on the South-Shore. Shallow water marine sediments sampled along the North-Shore depict a magnetic behavior and a mineralogical composition similar to the adjacent terrestrial coastal rocks. However, different properties can be observed in the deep marine Laurentian Channel (200-300 m) sediments with a decrease in quartz and an increase in mica and clay, as well a decrease in magnetic susceptibility compared to coastal sediments. These properties are also associated with a decrease in grain size, possibly reflecting weaker hydrodynamic conditions in the deep Laurentian Channel. On the other hand, the shallow water sediments sampled along the South-Shore are characterized by unexpected properties, with a mineralogical composition and magnetic properties closer to the composition of the North-Shore rather than the South-Shore source. This observation could reflect past or recent ice-rafting episodes which transported Precambrian material from the North to the South-Shore, as suggested by several previous studies highlighting a significant number of Precambrian blocs and pebbles along the South-Shore. Finally, our results suggest that the North-Shore is the primary source-area of present-day terrigenous sediments in the St. Lawrence Estuary, with the South-Shore contributing weakly to the global sedimentation. These observations are in general agreement with the present-day river discharges in the St. Lawrence Estuary, which are more important on the North-Shore than on the South-Shore.

Keywords : sediment, mineralogy, magnetism, provenance, St. Lawrence Estuary

TABLE DES MATIÈRES

LISTE DES TABLEAUX

LISTE DES FIGURES

INTRODUCTION GÉNÉRALE

Problématique

Une définition usuelle pour décrire un estuaire provient de Pritchard (1967) : « *An estuary is a semi-enclosed coastal body of water which have a free connection with the open sea and within which sea water is measurably diluted with fresh water derived from land drainage* ». Un estuaire se définit donc comme une zone de mélange entre le milieu terrestre et le milieu marin ouvert. Cette transition rapide entre ces deux domaines distincts se traduit par une variabilité drastique dans les processus physiques, chimiques et biologiques influençant directement la sédimentologie du milieu tel que les vitesses de sédimentation, la taille des grains, la nature du sédiment et les possibles structures sédimentaires associées (Dalrymple et Choi, 2007). De plus, les fortes vitesses de sédimentation en lien avec les apports terrigènes importants font de ces milieux de véritables archives climatiques à haute résolution (Dalrymple et al, 1992). Autrement dit, l'étude de la dynamique sédimentaire en milieu estuarien est riche en information, complexe et fera l'objet de ce mémoire. D'autre part, les études sur la provenance des sédiments sont elles aussi d'un grand intérêt en sédimentologie, car elles nous renseignent d'une part sur l'origine des sédiments, et d'autre part sur les conditions de transport et de déposition (e.g., Nesbitt et al., 1996; Morton and Hallsworth, 1999). Ce type d'études, en particulier l'approche quantitative, connaissent un véritable essor grâce à l'avancement des technologies (Welje and Eynatten, 2004). Dans ce contexte, la diffraction des rayons X (XRD) est reconnue comme un outil efficace pour identifier et quantifier l'assemblage minéralogique d'un échantillon brut de sédiments. Il s'agit donc d'une méthode performante pour les études de provenance (e.g., Eberl, 2004; Andrews et al., 2011; Dou et al., 2014). Moins communément utilisé, le magnétisme environnemental est également un outil efficace dans le traçage des sources de sédiments (e.g., Thompson and Oldfied 1986;

Maher and Thompson, 1999; Watkins and Maher, 2003; Zhang et al., 2008). Le magnétisme environnemental connait aujourd'hui un essor certain, car outre son efficacité, cette approche est non destructeur et relativement rapide (Liu et al., 2012). L'aspect non destructeur de la méthode est un point clé de cette maitrise : il favorise les approches « *multi-proxy* » malgré une quantité limitée de matériel et m'a permis de coupler la spécialité de deux de mes directeurs.

Le Saint-Laurent, un candidat d'exception

Les caractéristiques physiographiques de l'estuaire du Saint-Laurent font de ce système un candidat idéal pour une étude sur la provenance des sédiments. Premièrement, la zone d'étude (Figure 1) est bordée par deux formations géologiques différentes en âge et en composition. Au nord, le Bouclier canadien avec la province de Greenville (2,65 Ga à 970 Ma), et au Sud, la chaine des Appalaches (570 Ma à 275 Ma) (Piper et al., 1990). Cette opposition drastique est un atout précieux pour une étude de provenance, car les deux potentielles sources d'alimentation sont de natures et de lithologies différentes et sont donc théoriquement discriminables. Deuxièmement, le Saint-Laurent est caractérisé par une dynamique sédimentaire complexe favorisant les variations de composition associées au transport. Au sein de l'estuaire, les vitesses de sédimentation sont spatialement très variables : la tête du chenal Laurentien est une zone d'accumulation sédimentaire importante où les vitesses d'accrétion atteignent 0,70 cm/an (Smith et Schafer, 1999) et où une épaisse séquence sédimentaire de plus de 450 m a été identifiée (Duchesne et al., 2010). Ces vitesses sont ensuite réduites le long du chenal Laurentien et ne dépassent pas les 0,2 cm/an dans le golfe du Saint-Laurent. La granulométrie des sédiments de surface est également extrêmement variable reflétant l'impact marqué des processus hydrodynamiques et gravitaires (Pinet et al., 2011). L'estuaire est également caractérisé par une érosion côtière significative, de grands systèmes de dérive littorale (Bernatchez et Dubois, 2004; Bernatchez et al., 2012) et une prédisposition aux risques naturels (e.g., St-Onge et al., 2011). De plus, certains canyons et chenaux bordant la Côte-Nord exacerbent cette dynamique en favorisant le transfert de sédiments du domaine côtier au milieu marin

profond (Gagné et al., 2009; Normandeau et al., 2013). Par ailleurs, la grande amplitude thermique de l'eau de surface avec des températures inférieures à 0°C en hiver permet la création de glace de mer saisonnière (Saucier, 2003; de Vernal et al., 2011). Cette glace de mer peut déplacer des sédiments de toute taille allant du bloc métrique à l'argile et participe ainsi au budget érosion/déposition annuel (Dionne, 1988; Drapeau et al., 1990; Neumeier, 2011). Le retrait de l'Inlandsis laurentidien est un dernier attrait pour une étude sur le traçage des sources sédimentaires, car les icebergs ont transporté une grande quantité de matière précambrienne jusqu'à la Rive-Sud entre 10 000 et 13 000 avant aujourd'hui (e.g., Dionne et Potras, 1998., Dionne, 2007). La Rive-Sud devient donc également une source secondaire de matériel précambrien et peut possiblement les redistribuer vers le milieu marin. Finalement, ces deux principales sources potentielles sont drainées par des basins versants de tailles très différentes. Le débit total des rivières de la Côte-Nord étant beaucoup très supérieur au débit total des rivières de la Rive-Sud (Centre St-Laurent, 1996).

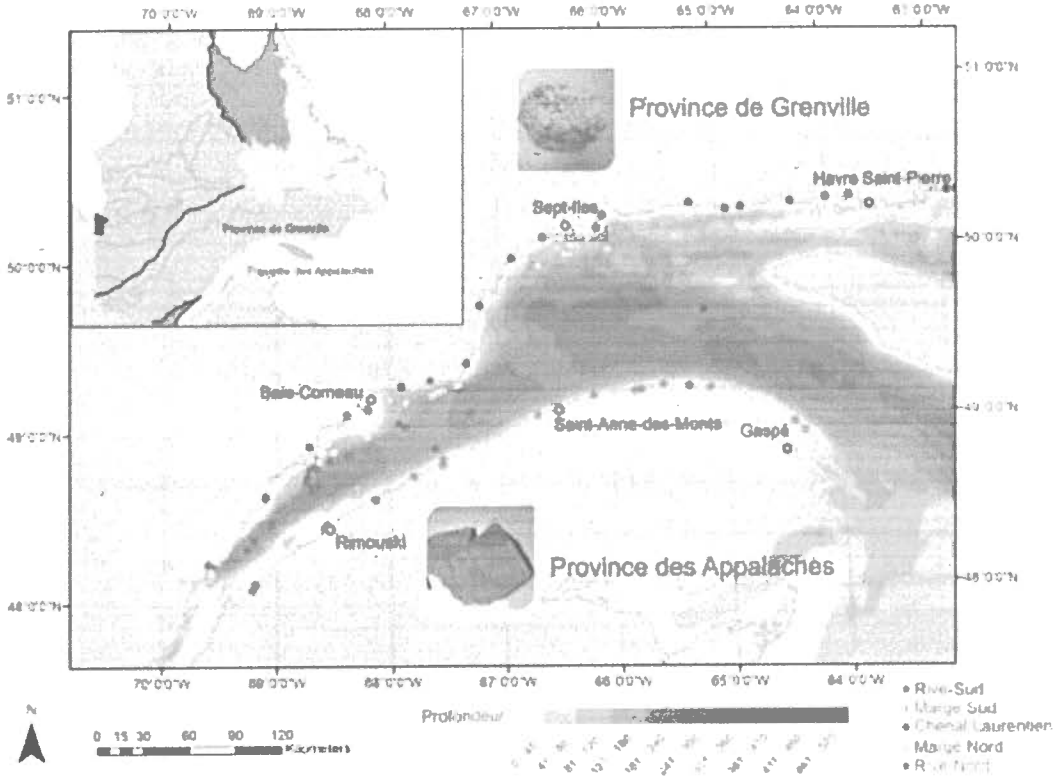

Figure 1. Localisation de la zone d'étude et des échantillons associés. L'ensemble des échantillons sont divisés en cinq régions : Côte-Nord (bleu foncé), Côte-Sud (vert foncé), Marge-Nord (bleu clair), Marge-Sud (vert clair), et chenal Laurentien (rouge). La zone d'étude est bordée par deux formations géologiques différentes. Au nord, le Bouclier canadien avec la province de Greenville (orange), et au Sud, la chaine des Appalaches (Jaune).

Objectifs

Considérant les caractéristiques sédimentaires actuelles de la zone d'étude et les géologies adjacentes, une étude sur la provenance des sédiments de l'estuaire est primordiale afin de caractériser les flux sédimentaires. L'objectif principal de cette maitrise est donc de déterminer la minéralogie et le comportement magnétique des sédiments de surface de l'estuaire du Saint-Laurent et de ses possibles sources adjacentes.

L'hypothèse à tester est que le couplage de données minéralogiques et magnétiques permet de discriminer l'opposition drastique entre le Bouclier canadien et les Appalaches ainsi que de caractériser la contribution de chacune de ces sources dans les sédiments de surface du chenal Laurentien et sur les marges adjacentes.

De façon plus spécifique, les objectifs sont de :

- Mesurer et analyser les propriétés magnétiques et la composition minéralogique des sédiments de surface des sédiments de l'estuaire du Saint-Laurent afin d'y déceler des variations spatiales;
- Mesurer et analyser les propriétés magnétiques et la composition minéralogique des sources potentielles de sédiments afin de les discriminer;
- Adapter et améliorer une méthode de traceurs basée sur la combinaison de la composition minéralogique et du comportement magnétique des sédiments pour caractériser les flux sédimentaires alimentant aujourd'hui l'estuaire du Saint-Laurent.

Organisation du mémoire et communications scientifiques

Ce mémoire est présenté sous la forme d'un article scientifique rédigé en anglais et qui sera soumis prochainement à la revue internationale *Marine Geology*.

Jaegle, M., St-Onge, G., Montero-Serrano, J-C., Lajeunesse, P. sera soumis prochainement. Tracing sediment sources in the St. Lawrence Estuary (eastern Canada) from mineralogical and magnetic signatures. *Marine geology.*

Par ailleurs, au cours de ma maîtrise, j'ai présenté mes travaux à quelques reprises aux congrès ci-dessous :

Jaegle, M., St-Onge, G., Lajeunesse, P., 2013. *Nature and origin of magnetic minerals present in the St. Lawrence Estuary*. Poster lors du congrès annuel des étudiants du GEOTOP, 1-3 février 2013, Wentworth-Nord, Qc.,Canada.

Jaegle, M., St-Onge, G., Montero-Serrano, J-C., Lajeunesse, P., 2014. *Tracing sediment sources in the St. Lawrence Estuary from mineralogical and magnetic signatures.* Présentation orale lors du congrès annuel des étudiants du GEOTOP, 14-16 mars 2014, Pohénégamook, Qc.,Canada.

Méthodologie et contribution

Campagnes d'échantillonnage

Contenu de son étendue spatiale, ce projet de maitrise m'a offert des opportunités de 5 campagnes d'échantillonnage. Au cours de l'été 2012, deux missions en mer auxquelles j'ai participé, ont été réalisées dans l'estuaire du Saint-Laurent afin d'échantillonner des sédiments de surface aux abords de la Côte-Nord. La première mission, à bord du N/R Coriolis II (Figure 2), m'a principalement permis de récolter des échantillons en milieu relativement profond. La deuxième mission à bord du N/R Louis-Edmond-Hamelin (Figure 3) m'a permis d'échantillonner des sédiments de surface en eau peu profonde à l'aide d'une benne grâce au faible tirant d'eau du navire. Au cours de l'été 2013, une nouvelle mission à bord du N/R Louis-Edmond-Hamelin m'a permis d'étoffer ma base de données. Cependant, les conditions de mer ayant été particulièrement difficile, cette troisième mission n'a pas permis d'échantillonner les sédiments tant convoités au large de la rivière Moisie et de récolter des données à l'aide du magnétomètre marin. J'ai également profité des missions stages de 2012 (en tant qu'étudiant) et de 2013 (en tant qu'auxiliaire d'enseignement) pour récolter de nouveaux échantillons de surface, notamment aux abords de la Rive-Sud. Finalement, deux campagnes d'échantillonnage en milieu terrestre ont été effectuées à l'été 2013 pour échantillonner les potentielles sources à l'embouchure des rivières le long de la Côte-Nord et de la Rive-Sud (Figure 4).

Figure 2. Navire de recherche Coriolis II.

Figure 3. Échantillonnage à bord du navire de recherche Louis-Edmond-Hamelin.

Figure 4. Vue d'une flèche littorale à l'embouchure d'une rivière de la Côte-Nord.

Analyses de laboratoire et contribution

L'ensemble des analyses de laboratoire ont été effectuées par mes soins à l'exception de 6 analyses granulométriques (MS11-17, MS11-19, MS11-20 MS11-23 MS11-24, MS11-25) effectuées par les étudiants de la mission stage de 2011. Les mesures granulométriques ont été réalisées à l'aide du granulomètre laser Beckman Coulter LS-13320 de l'ISMER. Les propriétés magnétiques ont été mesurées dans le laboratoire de paléomagnétisme du professeur Guillaume St-Onge à l'aide du magnétomètre cryogénique SRM-755 de *2G Enterprises*, du magnétomètre à gradient alternatif MicroMag 2900 de *Princeton Measurements Corp.* et de la sonde de susceptibilité magnétique *Bartington MS2*. La minéralogie par diffraction des rayons X a été réalisée dans le nouveau laboratoire du professeur Jean-Carlos Montero-Serrano avec un diffractomètre à rayons X PANalytical X'Pert. Finalement, la rédaction et l'ensemble des figures de l'article ont été réalisés par mes soins et révisés par mes trois codirecteurs et co-auteurs de cet article : Guillaume St-Onge (ISMER), Jean-Carlos Montero-Serrano (ISMER) et Patrick Lajeunesse (Université Laval).

Écoles d'été

Au cours de ces deux années de maitrise, j'ai également eu la chance de participer à des formations externes au programme. En 2012, j'ai participé à une école d'été internationale organisée par IODP/ECORD/GEOTOP à Montréal. Cette formation a permis de me familiariser avec les outils et techniques usuels en géologie marine. En 2013, j'ai suivi une formation organisée par l'Université de Minneapolis (États-Unis). Cette école d'été spécialisé en magnétisme environnemental m'a permis de développer des connaissances spécifiques dans ce domaine, me permettant ainsi de mieux appréhender mon sujet de maitrise. Outre les connaissances scientifiques acquises lors de ces formations, ces expériences ont été des opportunités uniques de rencontrer des chercheurs du monde entier travaillant avec les mêmes outils dans des projets connexes.

CHAPITRE 1

TRACING SEDIMENT SOURCES IN THE ST. LAWRENCE ESTUARY (EASTERN CANADA) FROM MINERALOGICAL AND MAGNETIC SIGNATURES

Matthieu Jaegle [1,3], Guillaume St-Onge [1,3], Jean-Carlos Montero-Serrano [1,3], Patrick Lajeunesse [2,3]

[1] Canada Research Chair in Marine Geology, Institut des sciences de la mer de Rimouski (ISMER), Université du Québec à Rimouski
[2] Centre d'études nordiques, & Département de géographie, Université Laval
[3] GEOTOP Research Center

Highlights

- First source to sink approach in the St. Lawrence Estuary and Gulf.
- Coupling of mineralogical composition, magnetic properties and grain size.
- Identification of the major sediment sources.

Abstract

Mineralogical composition, magnetic properties, and grain size distribution of surface sediment samples from the St. Lawrence Estuary (eastern Canada) were investigated in order to constrain present-day sediment provenance in the marine environment in agreement with the geological characteristics of the main rivers. The intercomparison of these properties and the application of principal component analysis enabled the discrimination of two distinct sources. The North-Shore source is characterized by increased feldspar content and high values of the magnetic properties such as magnetic susceptibility, anhysteretic, isothermal and saturated isothermal remanent magnetizations,

whereas the South -Shore source exhibits higher concentrations of phyllosilicates and quartz, and weaker magnetic property values. The discrimination of these two sources reflects the different bedrock lithologies predominant in both shores: (1) the Grenvillian metamorphic and igneous rocks of the Canadian Shield on the North Shore, and (2) the Early Palaeozoic sedimentary rocks belonging to the Appalachians Mountains on the South Shore. Shallow water marine sediments sampled along the North Shore depict a magnetic behavior and a mineralogical composition similar to the adjacent terrestrial coastal sediments. However, different properties can be observed in the deep marine Laurentian Channel (200-300 m) sediments with a decrease in quartz and an increase in mica and clay, as well a decrease in magnetic susceptibility compared to coastal sediments. These properties are also associated with a decrease in grain size, possibly reflecting weaker hydrodynamic conditions in the deep Laurentian Channel. On the other hand, the shallow water sediments sampled along the South Shore are characterized by unexpected properties, with a mineralogical composition and magnetic properties closer to the composition of the North Shore rather than the South-Shore source. This observation could reflect past or recent ice-rafting episodes which transported Precambrian material from the North to the South Shore, as suggested by several previous studies highlighting a significant number of Precambrian blocs and pebbles along the South Shore. Finally, our results suggest that the North Shore is the primary source-area of present-day terrigenous sediments in the St. Lawrence Estuary, with the South Shore contributing weakly to the global sedimentation. These observations are in general agreement with the present-day river discharges in the St. Lawrence Estuary, which are more important on the North Shore than on the South Shore.

1.1 INTRODUCTION

Tracing the provenance of sediments is one of the most studied subjects in sedimentology and is crucial to a complete understanding of the various factors controlling composition of basin fill, such as parent lithology, weathering, transport, and deposition of sediments (e.g, Nesbitt et al., 1996; Morton and Hallsworth, 1999). Moreover, the tracing of sources has been intensively developed due to advancements in measurement technology

(Welje and Eynatten, 2004). In this approach, X-ray diffraction (XRD) is a versatile technique to identify and quantify the mineral assemblages of matrix sediment samples. These mineralogical data are useful in determining the surface sediment provenance, sediment dispersal, and paleoclimate variability (e.g., Eberl, 2004; Andrews et al., 2013; Dou et al., 2014). In addition, bulk grain size analyses have also been used to decipher changes in sediment sources and transport processes (e.g., Xu et al., 2009; Andrews et al., 2011; Dietze et al., 2012; Hein et al., 2013; Andrews and Vogt, 2014). Similarly, previous studies have shown that the magnetic properties of the sediments can also be used to trace sediment sources (e.g., Thompson and Oldfield, 1986; Watkins and Maher, 2003; Zhang et al., 2008). Magnetic analyses of sediments are a powerful tool because the techniques are efficient, nondestructive, and sensitive to fine variation in mineralogy, concentration and grain size of magnetic minerals (Liu et al., 2012).

In this study, the mineralogical composition, magnetic properties, and grain size distribution of surface sediment samples from the St. Lawrence Estuary and Gulf (eastern Canada) and adjacent rivers were investigated and integrated in order to constrain present-day sediment provenance in this large marine system.

1.2 Geological setting

Geology

The St. Lawrence Estuary and Gulf is boarded by two distinct geologic provinces (Piper, 1990): the Greenville Province of the Canadian Shield to the North and the Appalachian Province to the South. These two geologic provinces are drastically different in age and petrographic composition. The Canadian Shield consists of Precambrian and Cambrian igneous and metamorphic rocks, whereas the Appalachians mainly consist of Paleozoic sedimentary rocks (Hocq, 1994 and Dubé, 1994). Moreover, according to the geological map of Quebec (Thériault and Beauséjour, 2012), the Greenville province is characterized by a medium to high degree of metamorphism and composed principally of

granitoids (granite, gneiss and migmatite), whereas the most common rocks on the South-Shore are sandstone, mudrock and conglomerate. In addition, there are many anorthosite intrusions in the Greenville province, which increases the variability of the study area (Hocq, 1994). The Sept-Îles area is for example one of the major intrusive suites in the Canadian Shield (Guillou-Frottier et al., 1995; Higgins and van Breemen, 1998; Higgins, 2005). The mafic Sept-Îles Intrusive Suite (SIIS) comprises the Precambrian and Cambrian igneous and metamorphic rocks of the Grenville province and is composed of anorthosite, gabbros, monzogabbros and other Fe–Ti oxide rocks. Moreover, a concentration of iron placers has been located in this area (Hein et al., 1993).

Sedimentology

The St. Lawrence Estuary and Gulf is a key location for paleoenvironmental reconstructions due to its very thick Quaternary sediment sequence and its position at the margin of the former Laurentide Ice Sheet during the last glaciation and deglaciation. (e.g., Syvitski and Praeg, 1989; de Vernal et al., 1996; Shaw et al., 2006; St-Onge et al., 2008; St-Onge and Long, 2009; Barletta et al., 2010; Duchesne et al., 2010). Also, these different glacial periods created a deep incision (>300 m) called the Laurentian Channel which incises the Estuary and Gulf from Tadoussac to the Cabot Strait (Figure 5). Today, this estuary is characterized by high sedimentation rates reaching 0.70 cm/yr at the head of Laurentian Channel (Smith and Schafer, 1999). Moreover, an increase in sedimentation rates is observed from the late Holocene to the present day (St-Onge et al., 2003). Likewise, significant coastal erosion and longshore drift are reported in various studies (Bernatchez et Dubois, 2004; Bernatchez et Fraser, 2012). Some submarine canyons and channels have been reported as contributing to sediment transport from the coast to the deeper marine environment (Gagné et al., 2009; Normandeau et al., 2013; Normandeau et al., 2014). The seafloor of the region is characterized by a great variability in grain size and landforms, including megadune and mass transport deposits (Pinet et al., 2011). The Laurentian Channel is mainly filled of fine silts, whereas its margins, in shallow water, are mainly

composed of coarser sediments varying from sands to fine silts. The grain size distribution of these sediments can be explained by the turbulence from the tides and waves which are stronger in shallow waters (Pinet et al., 2011). A first study about the provenance of surficial sediments by semi-quantitative X-ray analysis was conducted by Loring and Nota (1973). According to these authors, coarse surface sediments (>50 μm) of the Laurentian Channel system are essentially derived from the Canadian Shield and are mainly composed of plagioclase (44%), k-Feldspar (16%) and quartz (30%). Moreover, the St. Lawrence Estuary is prone to geohazards. Different geomorphological and geophysical evidence suggests the recurrence of slope instability and possible tsunamis throughout the Holocene (Cauchon-Voyer et al., 2008; 2011; Campbell et al., 2010; Poncet et al., 2010; St-Onge et al. 2011). Finally, sea ice is another parameter influencing the sedimentary dynamics. The St. Lawrence Estuary is considered as a sub-arctic region with temperatures below freezing during winter, allowing the formation of sea ice (Saucier, 2003; Anne de Vernal et al., 2011). Sea ice plays a major role in nearshore sediment dynamics in the estuary. It has the capacity to transport sediments of all sizes from clay to boulders and participates to the regional erosion budget (Drapeau et al., 1990). Studies have shown that the displacement of debris along the shore can be annual, even for boulders which can move for short distance (Dionne, 1988; Neumeier, 2011). Lithologic studies mentioned the great concentration of Precambrian boulders and pebble in the intertidal zone of the South-Shore of the estuary which implies that they have been ice-rafted from the North. Because most boulders are found in glacial marine clay deposits, the transport of these blocs and pebbles is related to active ice rafting episodes during the retreat of marine-based ice sheet whick took place in the region between 13 and 10 ka (Dionne 1998, 2007, Occhietti et al., 2011).

Hydrology

According to St. Lawrence Center (1996), large rivers from the North-Shore and the South-Shore contribute to the global water and sediment transport in the study area. Major difference in water discharge is noticeable between these two shores. The main rivers of the

North-Shore are characterized by a combined mean annual discharge of 3250 m^3/s of water, whereas on the South-Shore, combined annual mean discharge is only <150 m^3/s.

1.3 MATERIEL AND METHODS

Sample Collection

A total of 80 marine surface sediment samples were collected from the St. Lawrence Estuary (Figure 5 and Table in background dataset). The surface sediments were obtained from box core and Van Veen grab samplers. Occasionally, surface sediments were obtained from a trigger weight core when the surface was perfectly conserved. Surface samples were mainly sampled on board the R/V Coriolis II between 2002 and 2012, but some shallow water samples were collected from the R/V Louis-Edmond-Hamelin in the summers of 2012 and 2013. The sediments were collected at different depths and in different environments (coastal, deep marine, canyons). In order to identify the different sediment sources in the St. Lawrence Estuary and Gulf, 42 bedload samples were also collected at the mouth of all the rivers between Tadoussac and Natashquan for the North-Shore and between Trois-Pistoles and Gaspé for the South-Shore (Figure 5 and Table 1 in background dataset). Samples were collected near the mouths of rivers, where sediments represent a mixture of materiel from the drainage basin that is transferred to the marine environment. Some isolated samples also came from beaches. To avoid localized hydrodynamic effects, each sample consists of a combination of 4 or 5 sites that were spaced several tens of meters. The samples were divided into five regions according to their geographic position: (1) North-Shore and (2) South-Shore, corresponding to terrestrial and river sediments from the North and South geologic provinces; (3) North-Margin and (4) South-Margin, comprising relatively shallow marine sediments from either side of the Laurentian Channel; and (5) the Laurentian Channel, which includes deep water sediments in the Laurentian Channel itself.

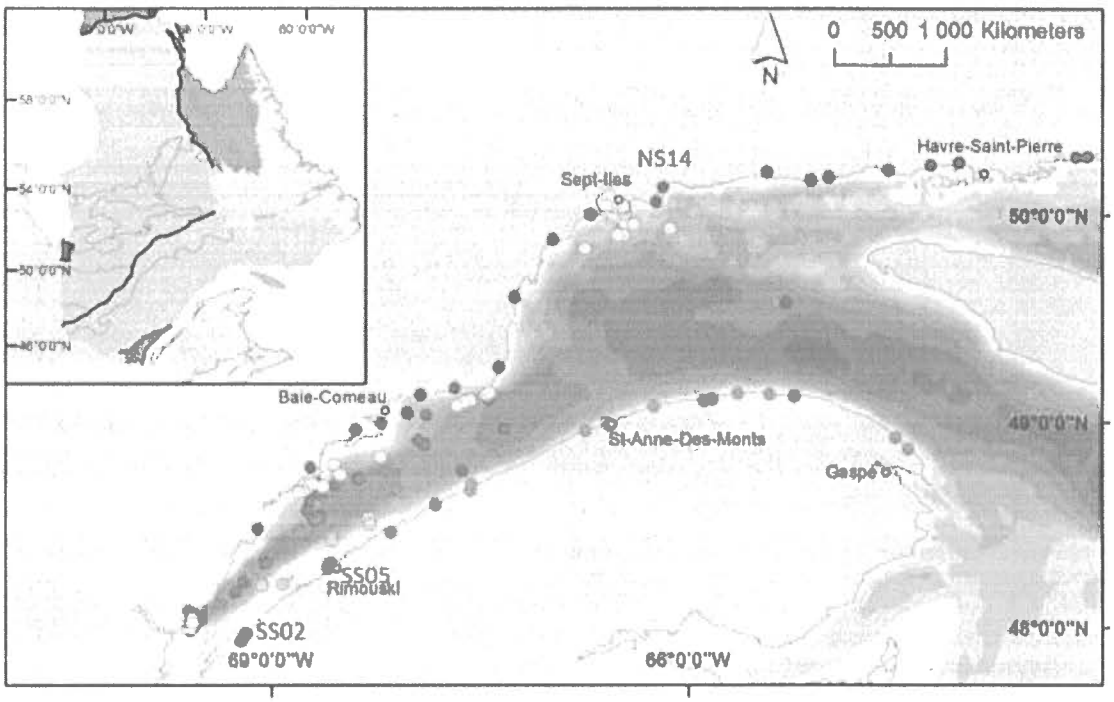

Figure 5. Location of the study area. All the samples were divided into five regions according to their geographic position: North-Shore (dark blue), South-Shore (dark green), North-Margin (light blue), South-Margin (ligth green), and the Laurentian Channel (red). The study area is boarded by two distinct geologic provinces with the Greenville province (Orange) in the North and the Appalachian province in the South (Yellow).

Analytical techniques

XRD measurements were carried out on bulk samples of terrestrial and marine sediments. Terrestrial sediments were also sieved at < 63 μm. This fraction was analyzed in order to gain a better understanding of grain size dependency. Before the bulk mineralogical analysis and in order to isolate the detrital fraction from the sediment samples, organic matter and biogenic carbonate were removed with 10 ml of peroxide and 10 ml of hydrochloric acid, respectively. Next, sediment samples were ground with a McCrone micronizing mill with agate grinding elements to obtain a consistent grain size of <10 μm by using 10 mL of ethanol and grinding times of 5-10 min to obtain a homogenous powder. The slurry was oven dried overnight at about 60°C and then slightly homogenized with an agate mortar to avoid the possible agglomeration of finer particles during drying. The random powder samples were side-loaded into the holders and analyzed by XRD using a PANalytical X'Pert Powder diffractometer. This instrument is fitted with a copper tube (Cu K-alpha = 1.54178Å), operating at 45 kV and 40 mA and a post-diffraction graphite monochromator. Samples were scanned from 5° to 65° two-theta in steps of 0.02° two-theta and a counting time of 2 seconds per step.

For the semi-quantification of the major mineralogical components, the bulk sediment XRD scans obtained were processed in the software package X'Pert High-Score Plus (PANalytical) using the Rietveld full-pattern fitting method. This method permits the semi-quantification of whole-sediment mineralogy with a precision of 5 – 10 % for phyllosilicates and 5 % for grain minerals. The quality of the Rietveld fitting procedure was evaluated for two statistical agreement indices: R-profile and goodness-of-fit (GOF). R-profile quantifies the difference between the observed and calculated patterns, whereas the GOF is the ratio between R-weighted profile (RWP; best least square fit between observed and calculated patterns) and R-expected theoretical (Rexp; best possible value for the residual). R-values profile between 20-30 % and GOF less than 3 are typically adequate in the Rietveld refinement of geological samples (e.g., Young, 1993). The major

mineralogical components that were quantified by this technique are: quartz, potassium feldspar (microcline + orthoclase), plagioclase feldspar (albite + anorthite), amphibole (hornblende), pyroxene (augite), magnetite, hematite, pyrite, and phyllosilicates (biotite, muscovite, illite, chlorite, smectite, and kaolinite). The phyllosilicates group can be separated into three sub-groups according to the basal spacing (or d-values) of the sheet silicate families: micas 10 Å (biotite, muscovite, illite), clay 14 Å (chlorite, smectite), and kaolinite 7 Å.

For magnetic measurements, samples were prepared by packing sediments into non-magnetic 8 cm^3 plastic cubes. Measurements of the low field volumetric magnetic susceptibility were carried out with a Bartington MS2 at low frequency (k_{lf}). Low frequency magnetic susceptibility is the most widely used magnetic property. This parameter reflects the contribution of different kind of magnetic behavior of minerals such as ferrimagnetic mineral (e.g., magnetite) antiferromagnetic minerals (e.g., hematite), paramagnetic minerals (e.g., silicate) and diamagnetic minerals (e.g. quartz). Low frequency susceptibility is thus an efficient proxy to observed variation in the magnetic concentration and composition of sediments (Liu et al., 2012). Different magnetic remanence measurements were also acquired in order to identify and characterize the magnetic concentration, mineralogy and grain size: anhysteretic remanent magnetization (ARM), isothermal remanence magnetization (IRM) and saturated isothermal remanent magnetization (SIRM) measurements. The ARM, IRM and SIRM were measured after progressive alternating field (AF) demagnetization from 0 to 80 mT in 5 mT steps using a 2G Enterprises SRM 755 cryogenic magnetometer. For susceptibility versus temperature experiments, a small quantity of sediment was air-dried before the measurement and measured using a Bartington MS2 high temperature apparatus. This measurement is used to determine the Curie temperature of the samples, which allows determining the mineralogy of the magnetic carrier (Tauxe, 2010). Finally, hysteresis properties were measured using an alternating gradient force magnetometer (AGM) MicroMag 2900 from Princeton Measurements Corporation on some representative samples. The shape of the loop and the derived properties (Ms, Mrs, Hc, Hcr) reflect the magnetic mineralogy, the domain state

and the magnetic particle size (Day et al., 1977; Tauxe, 2010). For hysteresis measurements, to obtain stable results, the coarse terrestrial sediments were previously sieved at 63 μm

Grain size analyses of sediment samples were performed with a Beckman Coulter LS13320 laser sizer on wet bulk sediment. Prior to measurement, sediments were sieved at 2 mm. The distribution parameters reported here - mean (μm), sorting and sediment grain-size composition (%) of clays (<2 μm), silts (2–63 μm), and sands (>63 μm) - were extracted using the GRADISTAT 4 software (Blott and Pye, 2001). Calculations were achieved using the geometric method of the moments.

Statistical approach: compositional biplot

The mineralogical data obtained are of a compositional nature, that is, they are vectors of non-negative values subjected to a constant-sum constraint. Namely, they are measured in units like wt.% (weight percent). This fact implies that relevant information is contained in the relative magnitudes, so statistical analysis must focus on the ratios between components (Aitchison, 1986). The suitability of the log-ratio approach for the analysis of data representing parts of a whole is supported from a theoretical viewpoint as well as from a practical one (see e.g., Weltje, 2002; von Eynatten, 2004; Barbera et al., 2009; Tolosana-Delgado and von Eynatten, 2009). The covariance biplot is used here as a graphical tool for exploring the relationships between the different variables and samples. The axes of the biplot correspond to the first two principal components (PCs) of the log-centered data, and both the samples and the components are simultaneously represented. Similar components are clustered together into a single part in the biplot. More details on the interpretation of a compositional biplot are discussed in von Eynatten et al. (2003) and Montero-Serrano et al. (2010). All statistical calculations (log-ratio transform and biplot) were conducted with "CoDaPack" software (Comas-Cufí and Thió-Henestrosa, 2011).

1.4 RESULTS

Sediment grain size

Sediment samples are characterized by unimodal or bimodal grain-size distribution in most cases. The sediment grain-size composition of all samples is illustrated on a ternary diagram (Figure 6). The Laurentian Channel margins depict a great variability and are mainly composed of sand to silt with mean values included between 10 μm and 480 μm. The grain size distribution of the Laurentian Channel sediments is more constant and mainly consits of fine silt with mean values ranging between 5 μm to 18 μm. Terrestrial sediments are relatively coarse and composed of sand and silt with mean values between 16 μm and 1000 μm.

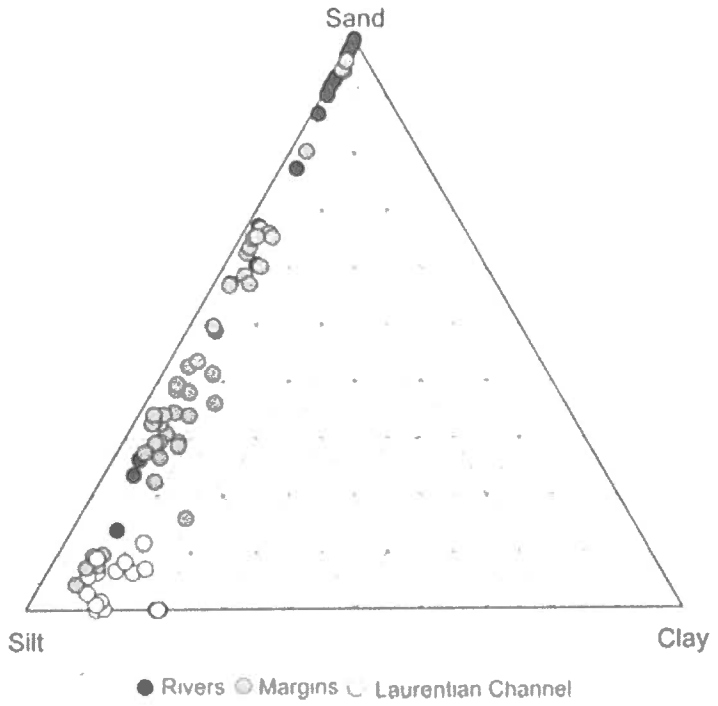

Figure 6. Sand, silt and clay ternary diagram of the studied surface sediments. The grain size distribution of the Laurentian Channel sediments consits of fine silt (white circles). Margins are composed of sand and silt (grey circles). River sediments consist of sand and coarse silt (black circles).

Bulk mineralogical composition

The five main minerals present in our samples are: quartz (15-59 %), potassium feldspar (1-22 %), plagioclase (12-65 %), mica (2-37 %), and clay (0-24 %). However, several other minerals were also frequently found in smaller quantities, such as pyroxene, amphibole, magnetite, hematite and calcium carbonate. Fe-Ti oxide content shows a high variability (0 % to 14 %), which will be discussed below (Figure 7). Biogenic carbonates were removed by acid treatment, while dolomite was not detected in the XRD diffractograms in the studied samples due to its low content. Figure 8 illustrates the spatial distribution of quartz, feldspar, clay and mica in the form of pie charts. To improve the readability some closely-spaced samples were removed. Great variability between the two shores and the deep marine environment areas can be observed and will be described below.

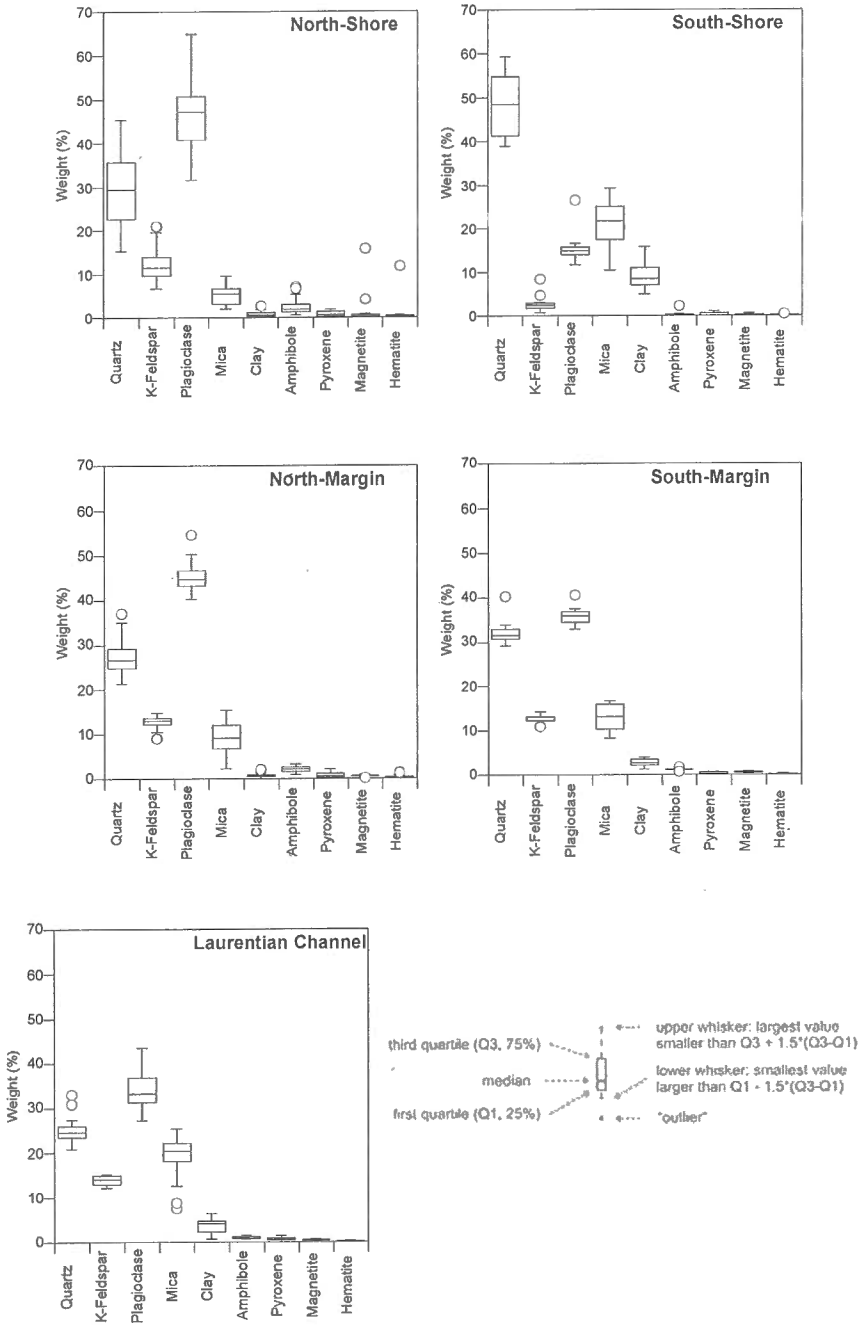

Figure 7. Box plots of the minerals present in the different regions (North-Shore, South-Shore, North-Margin, South-Margin, Laurentian Channel).

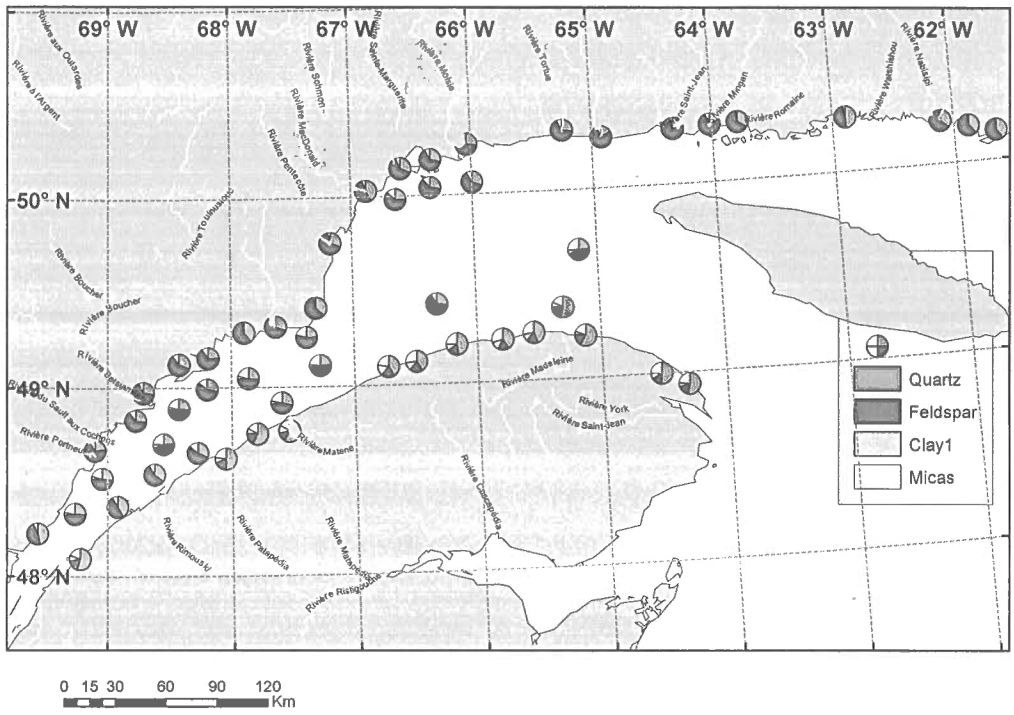

Figure 8. Map of pie charts for quartz, feldspar (alkali and plagioclase), mica and clay content in the St. Lawrence Estuary and Gulf. (Samples located too close to each other were removed to improve the lisibility of the figure and avoid overlapping of data.

Composition of the terrestrial samples

Box-plots of the 42 bedload river sediment samples reveal a drastic difference between the North and the South-Shores (Figure 7). Plagioclase and K-feldspar are more abundant along the North-Shore whereas clay, mica and quartz are more present along the South-Shore. Pyroxene, amphibole, magnetite and hematite are regularly present in limited percentages along the North-Shore and almost entirely absent from the South-Shore. To gain a better understanding of the mineral composition and to distinguish each shore, a principal component analysis (PCA) was conducted using the centered log-ratio method (Aitchison, 1986) (Figure 9). Only the five most dominant minerals (quartz, mica, clay, plagioclase and K-feldspar) were considered in this statistical approach. This analysis indicates that the PC1 is positively associated with clay and mica and negatively associated with K-feldspar and plagioclase, while the PC2 is negatively associated with quartz (Table 2). The PCA results clearly distinguish two clusters: the North-Shore and South-Shore sources. Greater K-feldspar and plagioclase content along the North-Shore and greater mica and clay content along the South-Shore is very pronounced along the PC1 and can be used to effectively distinguish the two sources. Moreover, comparison between the bulk and finer fraction along the PC2 reveals that the quartz content is slightly reduced for both shores in the <63 μm fraction.

Samples SS02 (muddy foreshore near Trois-Pistoles) and SS03 (tidal march near Rimouski) located on the South-Shore, are very interesting samples because they indicate a relative increase in total feldspar content and a relative decrease in total phyllosilicate and quartz content compared to the adjacent rivers (Figure 9). This composition approaches that of the North-Shore samples despite its geographic position. Unlike the other samples, these samples were not collected from a river or exposed beach, but rather from a muddy foreshore area. Similarly, sample SS05 (collected in a beach behind the tidal march of Rimouski) yield a similar situation with a composition more typical of the North-Shore samples.

Sample NS14 (Moisie River Delta) is another outlying sample, having a bulk composition rich in Fe-Ti oxides. NS14 has 15% of magnetite and 12% of hematite. Another sample (NS15) was collected 3 km upstream from the Moisie River Delta sample and its composition is totally different and shows a weak heavy mineral content, suggesting the increase in Fe-Ti oxides in the delta occurs over a short distance.

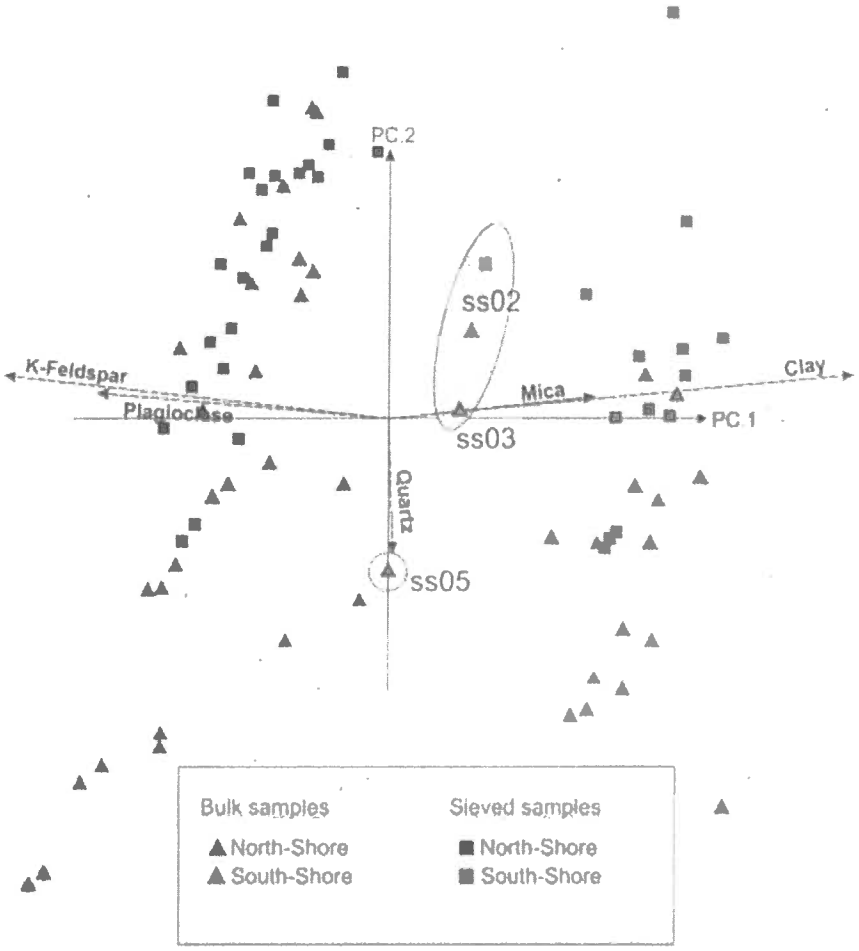

Figure 9. Biplot of the PC1 versus PC2 of the main minerals from the North-Shore and the South-Shore

Table 1. PCA scores for North-Shore and Souh-Shore samples

	Quatrz	K-spar	Plag	Mica	Clay	Cum.Prop.Exp.
PC1	0.0082	-0.5503	-0.4147	0.2949	0.6619	0.9113
PC2	-0.8896	0.2860	0.1431	0.2202	0.2403	0.9556

Composition of marine sediments and comparison with terrestrial sources

The PCA of the bulk mineralogical data of marine and terrestrial sediments also reveals several differences between the North and the South-Shores (Figure 10). Indeed, the PC1 is positively associated with K-feldspar and plagioclase and negatively associated with clay and mica, while the PC2 is negatively associated with quartz and positively associated with feldspar and clay (Table 3). Figure 10 illustrates a cluster of South-Shore sediments and a more extensive group, comprising North-Shore sediments, North-Margin sediments, South-Margin sediments and Laurentian Channel sediments, suggesting a relative similarity in composition between all these sectors compared to the South-Shore cluster. According to the PCA analyses and box plots (Figure 7 Figure 10), the North-Margin sediments depict a mineralogical composition similar to the adjacent terrestrial sediments. However, variations can be detected for the sediments farthest offshore, as illustrated by a decrease in quartz and plagioclase content, and an increase in mica content. K-feldspar content does not show clear variation, mean values are conserved. The same pattern of variation can be more easily observed in the deep marine Laurentian Channel sediments with a decrease in quartz and plagioclase content, and an increase in mica and clay content. South-Margin sediments are very close to those of the North-Margin in composition, with only a few samples showing relatively lower plagioclase content and relatively high mica content.

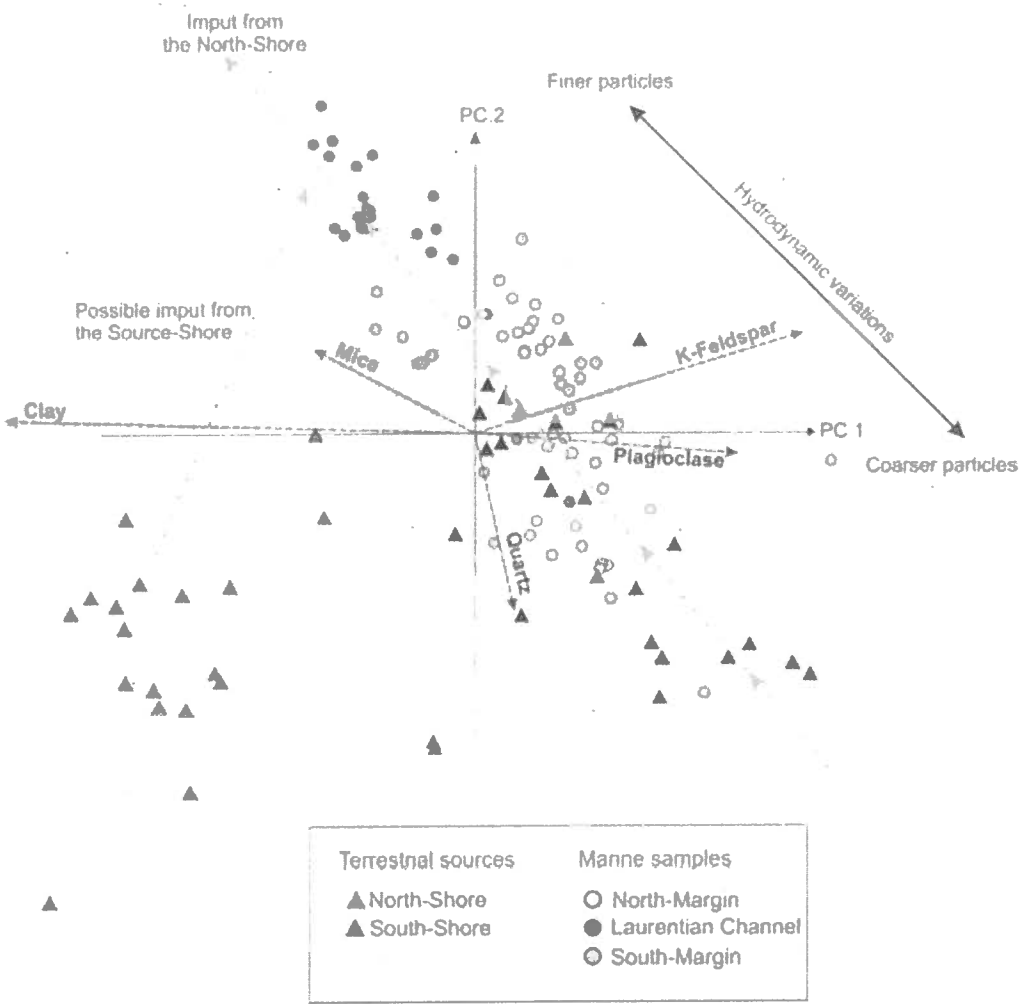

Figure 10. Biplot of the PC1 versus PC2 of the main minerals from The North-Shore, North Margin, Laurentian Channel, South Margin and South-Shore.

Table 2. PCA scores for all samples

	Quatrz	K-spar	Plag	Mica	Clay	Cum.Prop.Exp.
PC1	0.0730	0.4923	0.3935	-0.2169	-0.7419	0.8224
PC2	-0.8198	0.4689	-0.0618	0.3038	0.1089	0.9177

Magnetic properties

Magnetic properties are also used to distinguish significant differences between the two shores and the marine environment. According to the hysteresis loop from three representative samples (Figure 11), the assemblage of the magnetic grains of NS2 (North-Shore), SS4 (South-Shore) and COR0503-40 (Laurentian Channel) is dominated by low coercivity minerals as indicated by the saturation of the IRM acquisition below 300 mT. In addition, the thermomagnetic curve obtained from theses sample illustrates a sharp drop of magnetization at about 580°C which corresponds to the Curie temperature of magnetite (Figure 11), suggesting magnetite as the dominant magnetic carrier. A continuous loss in susceptibility is also visible from 300°C. This decrease in magnetic susceptibility from 300°C could be associated with the alteration of maghemite to hematite (Dearing, 1999). This is especially noted in Laurentian Channel sediment and South-Shore sediment because the magnetite signal is weaker. A Day-plot (Figure 12) is usually used to determine the domain state and magnetic grain size of samples (Day et al., 1977). In our study, because the terrestrial samples were sieved at 63 μm to obtain stable results with the alternating gradient force magnetometer, the results cannot be directly compared in terms of grain size changes with the other bulk samples from the marine environment. Nonetheless, Figure 12 reveals a trend where North-Margin and Laurentian Channel samples are perfectly aligned on a mixing line suggesting a common magnetic assemblage dominated by magnetite. South-Shore samples also show a trend, but it is slightly shifted to the right of the North-Margin/marine trend. This trend, along with the hysteresis loop and temperature experiment, indicate the predominance of magnetite as the main magnetic carrier, but the small shift hints at a minor contribution of other magnetic minerals for the southern sediments. Despite similarities in the magnetic assemblage for all sectors, ARM, IRM, SIRM, and k_{lf} are much lower in South-Shore rivers than in North-Shore rivers (Figure 13). This dissimilarity can reflect variations in concentration and grain size (Liu et al., 2012). Moreover, k_{lf} is not only affected by the ferrimagnetic content, but also by the concentration of antiferromagnetic (e.g., hematite), paramagnetic (e.g., silicate), and diamagnetic (e.g., quartz) minerals (Dearing, 1999). This dissimilarity is in accordance

with mineralogical results from this study where pyroxene and amphibole (paramagnetic) are more abundant along the North-Shore, while quartz is abundant along the South-Shore (diamagnetic). The magnetic susceptibility of the marine samples depicts a high variability with mean values close to North-Shore values (Figure 13). ARM, IRM and SIRM of the marine sediments are characterized by well-grouped data with mean values again close to the ones of the North-Shore sources (Figure 13). Despite the fact that magnetite dominates the mineral assemblage, unusual demagnetization curves/behavior with an increasing IRM over the first demagnetization few steps (Figure 14) is observed in samples collected in or near the Moisie River Delta. This remagnetization of the IRM during alternating field demagnetizaton is interpreted as a gyroremanent magnetization (GRM). A similar behavior was recently detected and interpreted as a pedogenic iron mineral signature such as hematite or goethite (Lisé-Pronovost et al., 2014). Similarly, GRM observed in the samples from the Moisie River delta suggests the presence of such high coercivity minerals in the assemblage. XRD data confirm this hypothesis in demonstrating the presence of hematite in sample NS14. In other cases, the concentration of high coercivity minerals is too low for XRD measurements and is only detected by magnetic analyses.

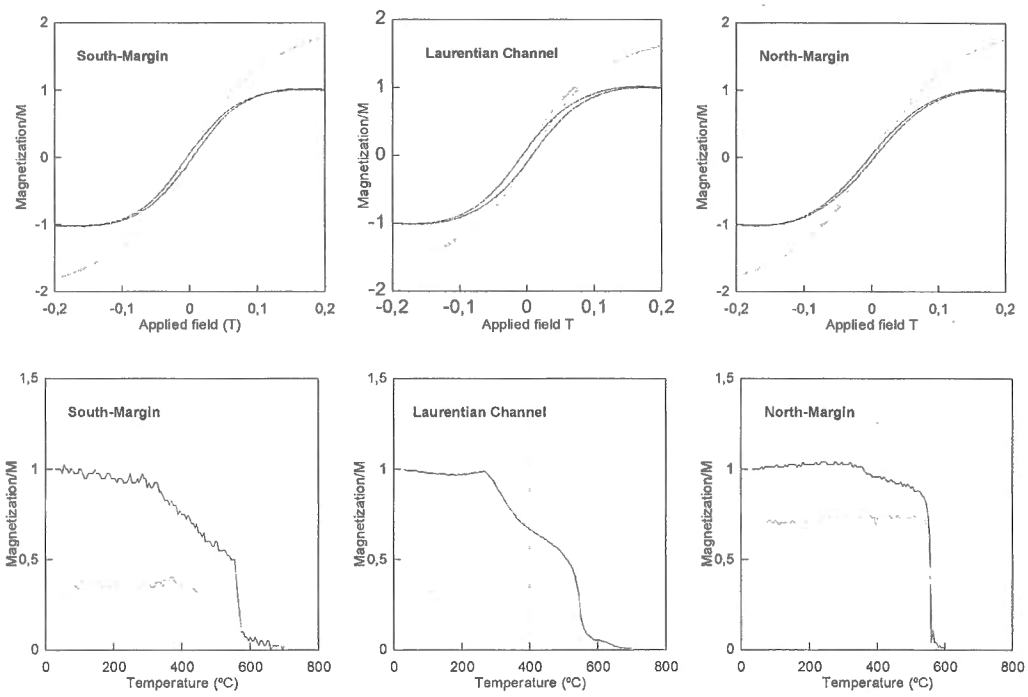

Figure 11. Hysteresis loops and high-temperature dependent magnetic susceptibility heating (black) and cooling (grey) curves for 3 representative samples in South-Margin sample, in Laurentian Channel sample and in North-Margin sample. For the hysteresis measurements, the grey curve reflects the raw data and the black curve the corrected data.

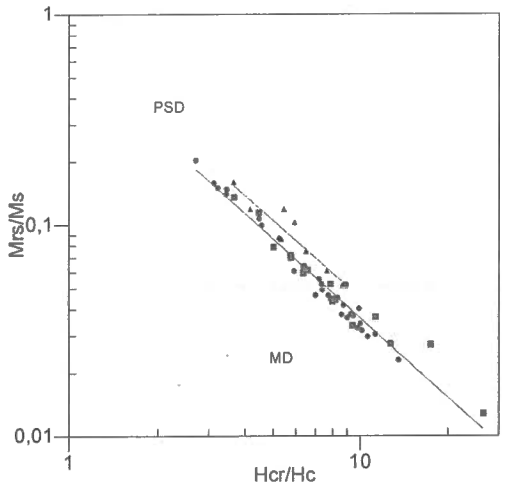

Figure 12. Day plot for North-Shore (dark blue), South-Shore (dark green), and all marine sediments (red). Adapted from Day (1977). North-Shore and marine samples are perfectly aligned on a mixing line suggesting a common magnetic assemblage.

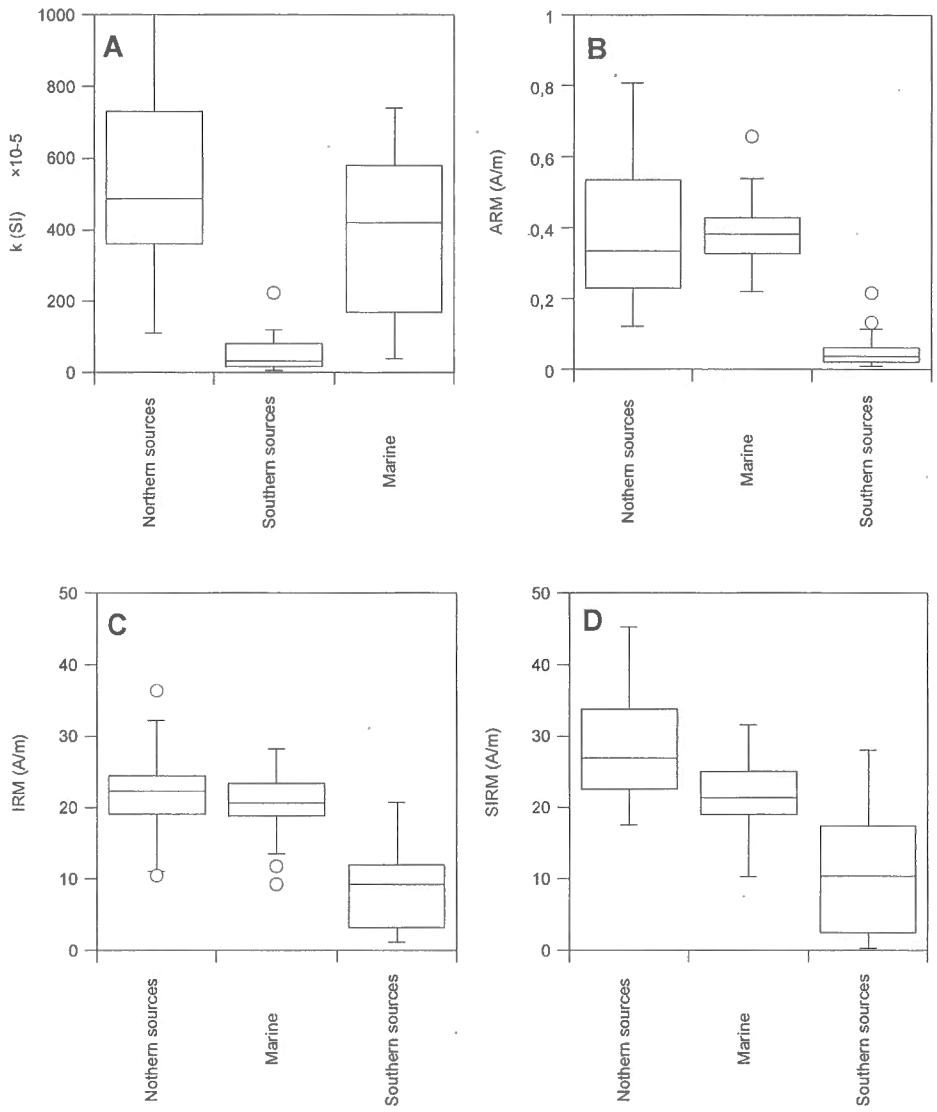

Figure 13. Comparison of the magnetic properties (k, ARM, IRM, SIRM) between the different environments. The North-Shore source is characterized by high values of the magnetic properties such as magnetic susceptibility, anhysteretic, isothermal and saturated isothermal remanent magnetizations, whereas the South-Shore exhibits weaker magnetic property values.

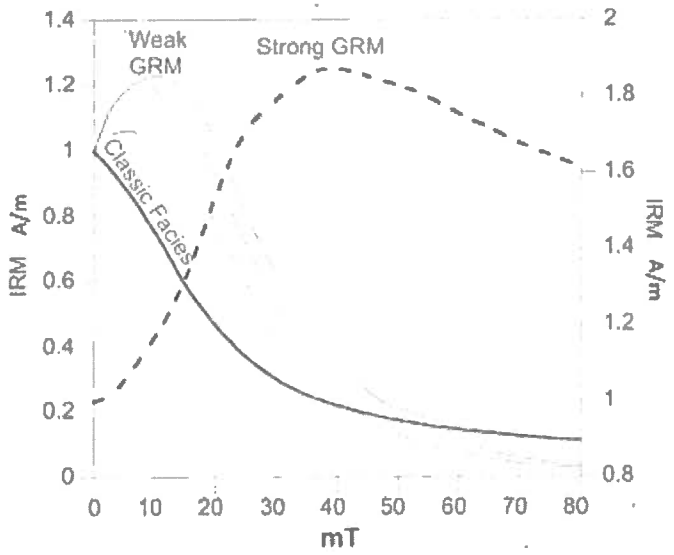

Figure 14. Comparison of IRM demagnetization curves. The red curve illustrates classical demagnetization facies in the study area. Black continued curves depict small gyroremanance for the Sept-Iles marine sediments, wheras the black dashed curve hints at a very strong GRM for the Moisie River Delta sediments.

Intercomparison of the bulk mineralogy, grain size and magnetic properties

One important aim of the present multi proxy analysis is the understanding of associations between all proxies. Therefore, the results of the PCA (Figure 1 and Table 2) were plotted versus grain size and magnetic susceptibility (Figure 15 a, b, c). Magnetic suceptibility was also compared to mean grain size in phi values (Figure 15d). PC2 is strongly correlated with grain size for all sediments regardless of the region (marine, North-Shore, South-Shore) (Figure 15). Variations of mineralogical composition along this axe are not dominated by the nature of sources but by variations of grain size between these different environments. On the other hand, the PC1 versus mean grain size plot (Figure 15b) illustrates a more complex behavior, but different tendencies can be distinguished in different regions: most notably, the PC1 correlates with mean grain size for marine samples, while terrestrial samples do not show any clear tendency. The composition along the PC1 is influenced by variations in source for terrestrial sediments, whereas it is mainly sensitive to grain size in marine environment. The comparison of grain size versus k_{lf} (Figure 15d) shows the same pattern, where the correlation is observed only for the marine samples, suggesting that k_{lf} is sensitive to variation of sources for terrestrial samples and is influenced by grain size in the marine environments. The PC1 is also well correlated with k_{lf} (Figure 15c) and highlights previous observations where South-Shore sediments have weaker magnetic susceptibility because the mineralogy, Laurentian Channel sediments too because the small size of particles, and North-shore sediments have stronger magnetic susceptibility because the mineralogy.

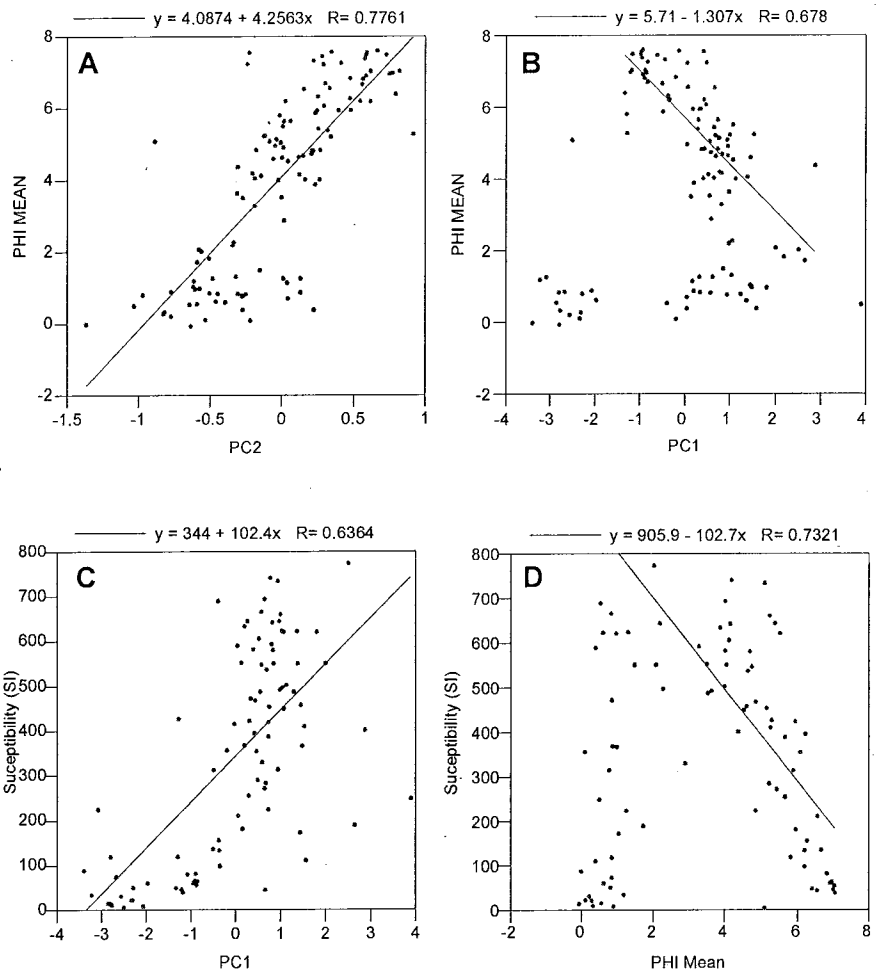

Figure 15. Intercomparison of marine (red), North-Shore (blue) and South-Shore (green) sediments. PC2 versus grain size (A); PC1 versus grain size (B); Grain size versus magnetic susceptibility (C); grain-size versus magnetic suceptibility (D). Regression lines and equations are calculated for all samples in A and C and for marine samples only in B and D.

1.5 Discussion

Two distinct sources related to the adjacent geology

The intercomparison of the sediment properties and the application of PCA enabled the discrimination of two distinct sources of supply. This discrimination reflects the different bedrock lithologies predominant on each shore: (1) the Grenvillian metamorphic and igneous rocks of the Canadian Shield on the North-Shore, and the (2) Early Palaeozoic sedimentary rocks belonging to the Appalachian Mountains on the South-Shore. The igneous and highly metamorphosed rocks of the Grenvillian province are responsible for the increase in feldspar, pyroxene and amphibole along the North-Shore. On the South-Shore, the sediment is mainly composed of sandstone, mudrock and conglomerate. These sedimentary rocks supply large quantities of fine-grained quartz and phylosillicates observed in the South-Shore samples. Similarly, the magnetic measurements (k_{lf}, ARM, IRM and SIRM) are also impacted by the two distinct geologic provinces. High values of the magnetic properties are associated with metamorphic and igneous rock samples from the North-Shore, which are characterized by a higher concentration of magnetic minerals and possible contribution of paramagnetic minerals such pyroxene and amphibole. Low values of magnetic properties are associated with southern sedimentary rocks with a weak concentration of magnetite and the contribution of diamagnetic minerals such as quartz. Location of the very high magnetic susceptibility, found along the North-Shore coincide with special mineralogical compositions rich in magnetite and hematite. The Moisie River Delta is a prominent example where the mafic Sept-Îles Intrusive Suite supplies a great quantity of Fe-Ti oxides and allows the formation of placers. Near Trois-Pistoles and Rimouski, feldspar enrichment and phyllosilicate impoverishment in samples SS02, SS03 (tidal marsh) and SS05 (beach) could reflect the impact of glacial legacy. Such as the Precambrian boulders and pebbles currently observed along the South-Shore (Dionne, 1998, 2007), these finer sediments (feldspar-rich) could represent past ice rafting episodes during deglaciation. The physiography of these sampling sites could justify the

conservation of Precambrian material compared to the other South-Shore sediments as samples SS02 and SS03 were sampled in weaker environments (tidal marsh), and site SS05 is protected by the St. Barnabé and Canuel islands.

Provenance of the marine sediments

The distribution of these sediments from two distinct sources (North-Shore and South-Shore) in surface sediments is a tool to understand the modern sedimentary transport or dynamics in the St. Lawrence Estuary. North-Margin sediments depict a bulk mineralogical composition similar to the adjacent terrestrial sediments (Figure 10). These shallow marine sediments generally derive from the adjacent coast by the rivers or/and beach erosion and retain their original terrestrial composition. Slight variations (decreasing of plagioclase and quartz, increasing of phyllosilicate) detected for the sediments farthest offshore are well correlated to grain size (Figure 10, Figure 15). These slight variations most likely reflect changes in hydrodynamic conditions, such as a decrease in the influence of currents and waves in the deeper environment (Pinet et al., 2011). The coarser and harder grains of quartz and plagioclase settle more rapidly and the lighter grains of mica and clay are transported over a longer distance. In addition to the positive correlation between mineralogical composition and grain size, preservation of K-feldspar excludes the possibility of variation in source because this mineral is almost absent on the South-Shore. Similarly, the variation in composition observed in the Laurentian Channel (a decrease in quartz and plagioclase accompanied by an increase in mica and clay) is also well correlated to the decrease in grain size (Figure 10 Figure 15), supporting weaker hydrodynamic conditions in the deep Laurentian Channel related to the greater depths (>300 m). As noted previously, the correlation between hydrodynamic conditions and mineralogical composition excludes major changes in the sediment sources; the most important part of sediments in the Laurentian Channel comes from the north. This asymmetry is consistent with previous oberservations (Loring and Nota, 1973).

These observations are in general agreement with the present-day river water discharges in the St. Lawrence Estuary, which are more voluminous on the North-Shore than on the South-Shore. However, despite the major fraction of sediments originating from the North-Shore in the Laurentian Channel, the increase in mica and clay observed in the Laurentian Channel could also reflects minor inputs from the South-Shore, which are rich in fine-grained sedimentary rocks such as mudrocks.

In constrast, the southern margin sediments sampled along the South-Shore are characterized by unexpected properties, with mineralogical compositions closer to those of the North-Shore than those of the South-Shore (Figure 10). Sediment supply in this sector is therefore not coming classically by the southern rivers and/or erosion of the South-Shore beaches, but by an indirect input from the North-Shore. This observation could reflect past or recent ice-rafting episodes which transported Precambrian material from the North-Shore to the South-Shore. Two hypotheses can potentially explain the input of Precambrian sediment is this area: (1) possible remobilization of old glacial deposits, rich in Precambrian materiel along the South-Shore, that crossed the St. Lawrence Estuary during the last glaciation/deglaciation. Samples SS02, SS03, SS05 are good examples of these secondary sources as they are characterized by an increase in feldspar (alkali and plagioclase) (2) present winter transport of Precambrian material across the St. Lawrence Estuary due to sea-ice rafting. Indeed, each winter a large part of the Estuary is covered by sea ice, but previous studies only focused on short distance transport along the coast. To our knowledge, long distance transport through the Estuary has not previously reported. Moreover, considering the sparse spatial distribution of our sampling along the South-Shore, this interpretation must be considered with caution: it could be a local effect and the entirety of the South-Shore is not necessary supplied by sea-ice rafting episodes. Figure 16 summarizes all these sources.

The magnetic approach also confirms the predominance of the northern sources in the composition of surface sediment in the Estuary and more particularly in the Laurentian Channel. The variability of k_{lf} and its good correlation with grain size in the marine

environment confirm that lower values of k_{lf} in the Laurentian Channel are not related to weak magnetic Paleozoic sediments, but are mainly influenced by finer Precambrian sediments aossociated to water depth conditions below 300 m water depth. Moreover, IRM and SIRM do not show a clear correlation with grain size in surface marine sediments of the Estuary. These parameters seem stable in marine environment excluding major source variation and confirming the dominance of the North-Shore.

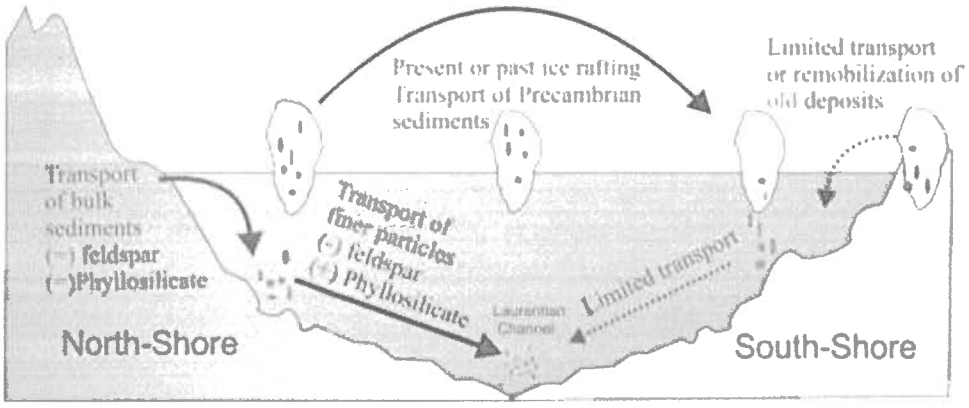

Figure 16. Synoptic sketch of the main sediment sources in the St Lawrence Estuary.

1.6 Conclusion

Study of mineralogical composition, magnetic properties and grain size distribution of surface sediments were realized for the first time in the St. Lawrence Estuary and Gulf in order to understand the distribution of sediments from both shores in the marine environment. Two main conclusions can be drawn from this paper:

(1) Mineralogical analyses and magnetic properties of terrestrial sediments were successfully used to identify two distinct sediment sources in the St. Lawrence Estuary and Gulf. The North-Shore source is characterized by increased feldspar content and high values of the magnetic properties such as magnetic susceptibility, anhysteretic, isothermal and saturated isothermal remanent magnetizations, whereas the South-Shore source exhibits a higher concentration of phyllosilicates and quartz, and weaker magnetic property values. The discrimination between these two sources reflects the different bedrock lithologies predominant in both shores;

(2) The marine sediments in the Laurenian Channel depict a magnetic behavior and a mineralogical composition closer to the composition of the North-Shore than the South-Shore. Mineralogical and magnetic variations such as a decrease of plagioclase, quartz and magnetic susceptibility, and an increase of phyllosilicate observed in the marine environment are well correlated to grain size and thus mainly related to hydrodynamic conditions and not to a source variation. In other words, the majority of the sediments in the Laurentian Channel are supplied by the North-Shore.

Also, transport by sea ice seems to play a significant role in the composition of surface sediments along the South-Margin. Unfortunately, discrimination between the role of present ice dynamics and ice rafted episodes during glaciation/deglaciation cannot be distinguished. A study investigating the present day role of sea ice in the regional sediment budget and sediment transport between the two coasts would for example allow determining the present role of ice in the transport of Precambrian material in this area.

Overall, this study lays the groundwork for futures studies using the mineralogical and magnetic signatures of sediment cores from the St. Lawrence Estuary and Gulf in order to reconstruct and document past variations in sediment inputs related to climate changes, particularly during the last glacial cycle when sediment inputs would have been different from those of today due to the presence of the Laurentide Ice Sheet which likely modified the erosional pattern.

CHAPITRE 2
CONCLUSION

Ce mémoire de maîtrise a permis pour la première fois de mener à terme une étude sur la nature et la provenance des sédiments présents dans l'estuaire et le golfe du Saint-Laurent et d'atteindre les objectifs de départ. L'utilisation de la diffraction des rayons X couplée au magnétisme environnemental a dans un premier temps permis de discriminer efficacement les deux principales sources potentielles de sédiments. La Côte-Nord est caractérisée par une forte proportion de plagioclases et de feldspaths alcalins. Bien que présents en proportion beaucoup plus faible, la présence de pyroxènes et d'amphiboles est récurrente dans l'ensemble des rivières de la Côte-Nord. La Rive-Sud se caractérise quant à elle par une forte concentration en quartz, en mica et en argile. Les feldspaths (alcalins et potassiques) sont retrouvés en proportion nettement plus faible que le long de la Côte-Nord. Les pyroxènes et les amphiboles sont totalement absents ou en quantité infime dans les sédiments de la Rive-Sud. Au niveau du magnétisme environnemental, la saturation de l'aimantation en dessous de 300 mT témoigne d'un assemblage magnétique dominé par des minéraux de faible coercivité pour les rivières de la Côte-Nord et de la Rive-Sud. La perte de l'aimantation à 580°C confirme que la magnétite est le minéral magnétique dominant dans le comportement magnétique. Bien que la magnétite soit présente de part et d'autre de l'estuaire, les mesures de la suceptibilité (k), de la magnétisation anhystérétique rémanente (ARM), de la magnétisation isothermale rémanente et isothermale rémanente de saturation (IRM et SIRM) et de la compilation des courbes d'hystérésis dans le diagramme de Day mettent en avant une différence entre les deux rives en lien avec la concentration en magnétite ainsi que l'effet des minéraux secondaires. La Côte-Nord est très riche en magnétite, entrainant des valeurs de susceptibilité, d'ARM, d'IRM, et de SIRM beaucoup plus élevées que le long de la Rive-Sud. Cette différenciation au niveau de la composition

minéralogique et de la réponse magnétique des deux sources est associée à la lithologie respective de chacune de ces côtes. Le Bouclier canadien avec ses roches ignées et métamorphiques est une source importante de feldspaths, de pyroxènes et d'amphibole. La grande quantité de fer dans ces mêmes roches est à l'origine de l'accroissement de l'aimantation des échantillons de la Côte-Nord. À l'inverse, les très nombreux affleurements de pélites, grès, ardoise et conglomérat des Appalaches produisent une grande quantité de phyllosilicate et de quartz. Le fer n'étant que peu présent dans ces roches, les valeurs de susceptibilité et d'aimantation sont nettement plus faibles.

L'analyse en composante principale de la composition minéralogie des données terrestres et des données marines apporte aussi une réponse tangible à la problématique de cette maîtrise. Deux groupes distincts se forment : le premier contient uniquement les échantillons terrestres de la rive Sud, alors que le second regroupe les échantillons terrestres de la Côte-Nord et l'ensemble des échantillons marins. Au sein de ce second groupe, les variations de composition minéralogique et de susceptibilité magnétique entre les sédiments des différents secteurs marins et ceux de la Côte-Nord sont relativement bien corrélées avec la variation de la taille des grains. La variation de proportion entre les feldspaths (-) et les phyllosilicates (+) en s'éloignant de la côte et dans le chenal Laurentien ne semble donc pas reliée à une contribution plus importante de la Rive-Sud malgré sa richesse en phyllosilicates, mais bien à un effet hydrodynamique. L'augmentation de la profondeur en s'éloignant de la côte diminue l'effet des vagues et des courants forçant la sédimentation des minéraux les plus grossiers et lourds (quartz, feldspath) au profil des minéraux plus légers (argiles, micas). Autrement dit, l'ensemble ou du moins la majeure partie des sédiments drapant le fond de l'estuaire proviendrait donc de la Côte-Nord. La différence de superficie entre les deux bassins versants concorde avec ces résultats. Les débits des rivières de la Côte-Nord sont bien supérieurs aux débits des rivières de la Rive-Sud. Par ailleurs, les sédiments recouvrant la marge sud montrent des résultats inattendus mais riche en information. Leur composition est relativement proche des sédiments de la marge nord. Ces échantillons ne seraient donc pas alimentés directement par les rivières et l'érosion des plages de la Rive-Sud, mais par une autre source de signature similaire à la

source Côte-Nord. Deux hypothèses pourraient expliquer cette signature particulière. (1) Il existe d'autres sources de sédiments précambriens le long de la Rive-Sud qui alimentent aujourd'hui la marge adjacente. L'échantillon SS02 serait un bon prétendant, mais la teneur en feldspath reste trop faible. Une nouvelle campagne d'échantillonnage serait nécessaire pour localiser et échantillonner ces possibles sources secondaires. (2) Aujourd'hui encore, ce secteur serait alimenté en sédiments par les glaces flottantes traversant l'estuaire pendant l'hiver. Pour cette seconde hypothèse, le transport glaciel est très bien documenté pour le transport local, mais le transport sur longue distance est à notre connaissance peu ou pas documenté dans l'estuaire et le golfe du Saint-Laurent. Il est important de prendre ces deux hypothèses avec précaution, car les échantillons provenant de la marge sud sont peu nombreux et spatialement regroupés.

Finalement, ces deux années de maîtrise ont donc permis de combler des lacunes dans les connaissances actuelles sur la provenance des sédiments de l'estuaire, mais elles apportent aussi de nouvelles questions et de nouvelles perspectives d'études. Il serait par exemple intéressant d'examiner en détail la dynamique sédimentaire de la Rive-Sud en milieu peu profond pour comprendre le transport des sédiments terrestres qui semblent peu ou ne pas alimenter l'estuaire bien que l'érosion côtière y soit présente (Bernatchez, 2004). Aussi, dans une optique paléo-environnementale, le projet de doctorat de Marie Casse (ISMER) apportera une réponse sur l'évolution de ce même schéma de provenance au cours des 8000 dernières années dans l'estuaire et le golfe du Saint-Laurent.

RÉFÉRENCES

Aitchison, J. (1986). *The statistical analysis of compositional data. Monographs on statistics and applied probability*. Chapman & Hall Ltd., London; reprinted in 2003 by the Blackburn Press, New Jersey, 416 p.

Andrews, J.T., Eberl, D.D., & Scott, D. (2011). Surface (sea floor) and near-surface (box cores) sediment mineralogy in Baffin Bay as a key to sediment provenance and ice sheet variations. *Canadian Journal of* Earth *Sciences, 48*, 1307–1328.

Andrews, J.T., Kristjánsdóttir, G.B., Eberl, D.D., & Jennings, A.E. (2013). A quantitative x-ray diffraction inventory of volcaniclastic inputs into the marine sediment archives off Iceland: A contribution to the Volcanoes in the Arctic System programme. *Polar Research, 32*, 11130.

Andrews, J.T. & Vogt, C. (2014). Source to sink: Statistical identification of regional variations in the mineralogy of surface sediments in the western Nordic Seas (58°N–75°N; 10°W–40°W). *Marine Geology, 357*, 151–162.

Barbera, G., Lo Giudice, A., Mazzoleni, P., Pappalardo, A., (2009). Combined statistical and petrological analysis of provenance and diagenetic history of mudrocks: application to Alpine Tethydes shales (Sicily, Italy). *Sedimentary. Geology, 213*, 27–40.

Barletta, F., St-Onge, G., Stoner, J. S., Lajeunesse, P., & Locat, J. (2010). A high-resolution Holocene paleomagnetic secular variation and relative paleointensity stack from eastern Canada. *Earth and Planetary Science Letters, 298*, 162–174.

Bernatchez, P. & Dubois, J.M. (2004). Bilan des connaissances de la dynamique de l'érosion des côtes du Québec maritime laurentien. *Géographie physique et Quaternaire, 58*, 45–71.

Bernatchez, P. & Fraser, C. (2012). Evolution of coastal defence structures and consequences for beach width trends, Québec, Canada. *Journal of Coastal Research, 285*, 1550–1566.

Blott, S.J. & Pye, K. (2001). Gradistat: a grain size distribution and statistics package for the analysis of unconsolidated sediments. *Earth Surface Processes and Landforms 26*, 1237–1248.

Campbell, C. D., Duchesne, M., & Bolduc, A. (2008). Geomorphological and geophysical evidence of Holocene seafloor instability on the southern slope of the Lower St. Lawrence estuary, Québec. *Proceedings .,of the 4th Canadian Conference on Geohazards : From Causes to Management* ed J Locat, D Perret, D Turmel, D Demers and S Leroueil (Québec: Presse de l'Université Laval), 367-374.

Cauchon-Voyer, G., Locat, J., & St-Onge, G. (2008). Late-Quaternary morpho-sedimentology and submarine mass movements of the Betsiamites area, Lower St. Lawrence Estuary, Quebec, Canada. *Marine Geology, 251*, 233–252.

Cauchon-Voyer, G., Locat, J., Leroueil, S., St-Onge, G., & Demers, D. (2011). Large-scale subaerial and submarine Holocene and recent mass movements in the Betsiamites area, Quebec, Canada. *Engineering Geology, 121*, 28–45.

Comas-Cufí M, Thió-Henestrosa S. (2011). *CoDaPack 2.0: a stand-alone, multi-platform compositional software.* In: Egozcue JJ, Tolosana-Delgado R, Ortego MI, eds. CoDaWork'11: 4th International Workshop on Compositional Data Analysis. Sant Feliu de Guíxols.

Thériault, R., & Beauséjour, S. (2012). Carte géologique du Québec. Ministère des Ressources naturelles. Québec. DV 2012-06. 1/mnhj250 000.

Day, R., Fuller, M., & Schmidt, V.A. (1977). Hysteresis properties of titanomagnetites: Grain-size and compositional dependence. *Physics of the Earth and Planetary Interiors, 13*, 260–267.

Dalrymple, R.W., & Choi, K. (2007). Morphologic and facies trends through the fluvial–marine transition in tide-dominated depositional systems: A schematic framework for environmental and sequence-stratigraphic interpretation. *Earth-Science Reviews, 81*, 135–174.

Dalrymple, R.W., Zaitlin, B.A., & Boyd, R. (1992). Estuarine facies models: conceptual basis and stratigraphic implications. *Journal of Sedimentary Research, 62*, 1130–1146.

Dearing, J.A. (1999). *Environmental Magnetic Susceptibility: Using the Bartington MS2 System*. Chi Pub., Kenilworth, 54p.

de Vernal, A., Hillaire-Marcel, C., & Bilodeau, G. (1996). Reduced meltwater outflow from the Laurentide ice margin during the Younger Dryas. *Nature, 381*, 774–777.

de Vernal, A., St-Onge, G., & Gilbert, D. (2011). Oceanography and Quaternary geology of the St. Lawrence Estuary and the Saguenay Fjord. *IOP Conference Series: Earth and Environmental Science*, *14*, 012004.

Dietze, E., Hartmann, K., Diekmann, B., IJmker, J., Lehmkuhl, F., Opitz, S., Stauch, G., Wünnemann, B., Borchers, A. (2012). An end-member algorithm for deciphering modern detrital processes from lake sediments of Lake Donggi Cona, NE Tibetan Plateau, China. *Sedimentary Geology*, *243-244*, 169–180.

Dionne, J.-C. (1988). Ploughing boulders along shorelines, with particular reference to the St. Lawrence estuary. *Geomorphology*, *1*, 297–308.

Dionne, J.-C. & Poitras, S. (1998). Lithologie des cailloux de la baie de Mitis, rive sud de l'estuaire maritime du Saint-Laurent (Québec) : un exemple de transport glaciaire et glaciel complexe. *Géographie physique et Quaternaire*, *52*, 107–122.

Dionne, J.-C. (2007). La batture de l'anse au Sable à Rimouski : un estran typique de la rive sud de l'estuaire maritime du Saint-Laurent, Québec. *Géographie physique et Quaternaire*, *61*, 195–210.

Dou, Y., Li, J., Zhao, J., Wei, H., Yang, S., Bai, F., & Wang, L. (2014). Clay mineral distributions in surface sediments of the Liaodong Bay, Bohai Sea and surrounding river sediments: Sources and transport patterns. *Continental Shelf Research*, *73*, 72–82.

Drapeau, G., (1990). Nearshore sediment dynamics in the St. Lawrence estuary. In: El-Sabh and Silverberg (Eds.), *Oceanography of a Large-scale Estuarine System. The St. Lawrence*. Springer-Verlag, New York, pp. 130-154.

Duchesne, M. J., Pinet, N., Bédard, K., St-Onge, G., Lajeunesse, P., Campbell, D. C., & Bolduc, A. (2010). Role of the bedrock topography in the Quaternary filling of a giant estuarine basin: the Lower St. Lawrence Estuary, Eastern Canada. *Basin Research*, 1–19.

Eberl, D.D. (2004). Quantitative mineralogy of the Yukon River system: Changes with reach and season, and determining sediment provenance. *American Mineralogist*, *89*, 1784–1794.

Gagné, H., Lajeunesse, P., St-Onge, G., & Bolduc, A. (2009). Recent transfer of coastal sediments to the Laurentian Channel, Lower St. Lawrence Estuary (Eastern Canada), through submarine canyon and fan systems. *Geo-Marine Letters*, *29*, 191–200.

Guillou-Frottier, L., Mareschal, J.C., Jaupart, C., Gariépy, C., Lapointe, R., & Bienfait, G. (1995). Heat flow variations in the Grenville Province, Canada. *Earth and Planetary Science* Letters, 136, 447–460.

Hein, F.J., Syvitski, J.P.M., Dredge, L.A., & Long, B.F. (1993). Quaternary sedimentation and marine placers along the North-Shore, Gulf of St. Lawrence. *Canadian Journal of Earth Sciences, 30*, 553–574.

Hein, J.R., Mizell, K., & Barnard, P.L. (2013). Sand sources and transport pathways for the San Francisco Bay coastal system, based on X-ray diffraction mineralogy. *Marine Geology, 345*, 154–169.

Higgins, M.D., & Van Breemen, O. (1998). The age of the Sept Iles layered mafic intrusion, Canada: implications for the late neoproterozoic/Cambrian history of southeastern Canada. *Journal of Geology, 106*, 421–431.

Higgins, M.D. (2005). A new interpretation of the structure of the Sept Iles Intrusive suite, Canada. *Lithos, 83*, 199–213.

Hocq, M. Dubé, C. (1994). *Géologie du Québec*. Les Publications du Québec, Québec, 154 p.

Loring, D.H., & Nota, D.J.G. (1973). *Morphology and sediments of the Gulf of St. Lawrence*. Bulletin of the Fisheries Research Board of Canada, Ottawa, v.182, 147 p.

Liu, Q., Roberts, A.P., Larrasoaña, J.C., Banerjee, S.K., Guyodo, Y., Tauxe, L., & Oldfield, F. (2012). Environmental magnetism: Principles and applications. *Reviews of Geophysics, 50*.

Lisé-Pronovost, a., St-Onge, G., Gogorza, C., Jouve, G., Francus, P., & Zolitschka, B. (2014). Rock-magnetic signature of precipitation and extreme runoff events in south-eastern Patagonia since 51,200 cal BP from the sediments of Laguna Potrok Aike. *Quaternary Science Reviews, 98*, 110–125.

Maher, B. A., & Thompson, R. (1999). *Quaternary Environments, Climates and Magnetism*. Cambridge University Press, Cambridge, 391p.

Montero-Serrano, J. C., Palarea-Albaladejo, J., Martín-Fernández, J. a., Martínez-Santana, M., & Gutiérrez-Martín, J. V. (2010). Sedimentary chemofacies characterization by means of multivariate analysis. *Sedimentary Geology, 228*, 218–228.

Morton, A. C., & Hallsworth, C. R. (1999). Processes controlling the composition of heavy mineral assemblages in sandstones. *Sedimentary Geology, 124*, 3–29.

Nesbitt, H.W., Young, G.M., McLennan, S.M., & Keays, R.R. (1996). Effects of chemical weathering and sorting on the petrogenesis of siliciclastic sediments, with implications for provenance studies. *Journal of Geology, 104*(5), 525–542.

Normandeau, A., Lajeunesse, P., & St-Onge, G. (2013). Shallow-water longshore drift-fed submarine fan deposition (Moisie River Delta, Eastern Canada). *Geo-Marine Letters, 33*, 391–403.

Normandeau, A., Lajeunesse, P., St-Onge, G., Bourgault, D., Drouin, Ş. S.-O., Senneville, S., & Bélanger, S. (2014). Morphodynamics in sediment-starved inner-shelf submarine canyons (Lower St. Lawrence Estuary, Eastern Canada). *Marine Geology, 357*, 243–255.

Neumeier, U. (2011). Boulder transport by ice on a St. Lawrence salt-marsh, pattern of pluriannual movements. *Proceedings of the Coastal Sediments, 11*, 2533–2545.

Occhietti, S., Parent, M., Lajeunesse, P., Robert, F., & Govare, É. (2011). Late Pleistocene–Early Holocene Decay of the Laurentide Ice Sheet in Québec–Labrador. *Developments in Quaternary Sciences,15*, 601–630.

Pinet, N., Brake, V., & Campbell, C. (2011). Seafloor and Shallow Subsurface of the St. Lawrence River Estuary, *Geoscience Canada 38,* 31–40.

Piper, D.J.W., Mudie, P.J., Fader, G.B., Josenhans, H.W., MacLean, B., Vilks, G., 1990. Quaternary geology, chapter 10. In: Keen, M.J., Williams, G.L. (Eds.), Geology of the Continental Margin of Eastern Canada. Geological Survey of Canada, , pp. 475–607

Pritchard, D.W. (1967). What is an estuary: physical viewpoint. In: Lauf, G. H. (Ed.) Estuaries. A.A.A.S. Publ. 83. Washington, DC. pp. 3–5.

Saucier, F. J. (2003). Modeling the formation and circulation processes of water masses and sea ice in the Gulf of St. Lawrence, Canada. *Journal of Geophysical Research, 108*(C8), 3269.

Shaw, J., Piper, D.J.W., Fader, G.B.J., King, E.L., Todd, B.J., Bell, T., Batterson, M.J., Liverman, D.G.E. (2006). A conceptual model of the deglaciation of Atlantic Canada. *Quaternary Science Reviews, 25*, 2059–2081.

Smith, J.N., & Schafer, C.T. (1999). Sedimentation, bioturbation, and Hg uptake in the sediments of the estuary and Gulf of St. Lawrence. *Limnology and Oceanography, 44*, 207–219.

St. Lawrence Center. (1996). State of the Environment Report on the St. Lawrence River. Volume 1: The St. Lawrence Ecosystem. "St. Lawrence UPDATE" series. Environment Canada – Quebec Region, Environmental Conservation, and Éditions MultiMondes. Montreal,

St-Onge, G., Stoner, J. S., & Hillaire-Marcel, C. (2003). Holocene paleomagnetic records from the St. Lawrence Estuary, eastern Canada: Centennial- to millennial-scale geomagnetic modulation of cosmogenic isotopes. *Earth and Planetary Science Letters*, *209*(1-2), 113–130.

St-Onge, G., Lajeunesse, P., Duchesne, M. J., & Gagné, H. (2008). Identification and dating of a key Late Pleistocene stratigraphic unit in the St. Lawrence Estuary and Gulf (Eastern Canada). *Quaternary Science Reviews*, *27*, 2390–2400.

St-Onge, G., & Long, B.F. (2009). CAT-scan analysis of sedimentary sequences: An ultrahigh-resolution paleoclimatic tool. *Engineering Geology*, *103*, 127–133.

St-Onge, G., Duchesne, M.J., & Lajeunesse, P. (2011). Marine geology of the St. Lawrence Estuary. *IOP Conference Series: Earth and Environmental Science*, *14*, 012003.

Syvitski, J.P.M., & Praeg, D.B. (1989). Quaternary Sedimentation in the St. Lawrence Esturary and Adjoining Areas, Eastern Canada: An Overview Based on High-Resolution Seismo-Stratigraphy. *Géographie Physique et Quaternaire*, *43*, 291–310.

Tauxe, L., (2010). *Essentials of Paleomagnetism*. University of California Press. San Diego. 513 p.

Thompson, R., & Oldfield, F., (1986). *Environmental Magnetism*. Allen and Unwin. London, 227 p.

Tolosana-Delgado, R., von Eynatten, H., (2009). Grain-size control on petrography composition of sediments: compositional regression and rounded zeros. *Mathematic Geoscience, 41*, 869–886.

von Eynatten, H., Barceló-Vidal, C., Pawlowsky-Glahn, V., (2003). Sandstone composition and discrimination: a statistical evaluation of different analyticalmethods. *Journal of Sedimentary Research, 73*, 47–57.

von Eynatten, H. (2004). Statistical modelling of compositional trends in sediments. *Sedimentary Geolology, 171*, 79–89.

Watkins, S., & Maher, B. (2003). Magnetic characterisation of present-day deep-sea sediments and sources in the North Atlantic. *Earth and Planetary Science Letters, 214*, 379–394.

Weltje, G. J. (2002). Quantitative analysis of detrital modes: statistically rigorous confidence regions in ternary diagrams and their use in sedimentary petrology. *Earth-Science Review, 57*, 211–253.

Weltje, G.J., & von Eynatten, H. (2004). Quantitative provenance analysis of sediments: review and outlook. *Sedimentary Geology, 171*, 1–11.

Xu, K., Milliman, J.D., Li, A., Liu, P., Kao, S.-J., & Wan, S. (2009). Yangtze- and Taiwan-derived sediments on the inner shelf of East China Sea. *Continental Shelf Research, 29*, 2240–2256.

Young, R. A. (1993). *The Rietveld Method. International Union of Crystallography Monographs on Crystallography 5*. [Chester, England]: Oxford; New York: International Union of Crystallograhy; Oxford University Press, 308p.

Zhang, W., Xing, Y., Yu, L., Feng, H., & Lu, M. (2008). Distinguishing sediments from the Yangtze and Yellow Rivers, China: a mineral magnetic approach. *The Holocene, 18*, 1139–1145.

Background dataset

ID	y	x	Secteur	Type	Sand	Silt	Clay	Mean	Quartz	k-Feldspar	Plagioclase	Feldspar	Amphibole	Pyroxene	Magnetite	Hematite	Micas	Clay	k	ARM	IRM
CN1306-03	48.1317	-69.1848	North-Shore	Bulk	1.0000	0.0000	0.0000	655.2103	30.43	13.54	50.79	64.33	0.86	0.83	0.3	0.01	2.2	0.49	622	0.378	13.489
CN1306-04	48.2413	-69.5980	North-Shore	Bulk	0.2366	0.7178	0.0455	24.4025	22.89	18.03	48.82	66.85	1.6	0.01	0.25	0.01	6.76	1.01	284	0.166	11.045
CN1306-05	48.2291	-69.5537	North-Shore	Bulk	0.9268	0.0679	0.0054	474.1862	45.25	11.48	33.66	45.14	1.16	0.43	0.21	0.09	5.95	1.08	472	0.335	15.604
CN1306-06	48.6435	-69.0987	North-Shore	Bulk	NaN	NaN	NaN	NaN	21.01	14.88	49.53	64.41	2.18	1.55	0.77	0.21	8.4	0.36	487	0.536	18.439
CN1306-07	48.9442	-68.7111	North-Shore	Bulk	0.4893	0.4667	0.0440	39.2092	25.26	14.01	48.12	62.13	2.29	1.84	0.16	0.22	6.9	0.5	449	0.377	19.092
CN1306-08	49.1255	-68.3757	North-Shore	Bulk	0.6059	0.3460	0.0481	53.3060	29.37	9.54	45.24	54.78	2.59	1.53	0.53	0.15	9.56	0.73	605	0.230	21.958
CN1306-09	49.1580	-68.1869	North-Shore	Bulk	0.9720	0.0251	0.0028	505.4204	23.15	9.91	51.34	61.25	3.8	0.01	0.13	0.38	9.07	1.22	368	0.231	24.339
CN1306-10	49.2918	-67.8949	North-Shore	Bulk	0.9314	0.0628	0.0057	401.1955	37.55	11.92	44.65	56.57	1.24	0.87	0.32	0.18	2.74	0.36	173	0.157	19.341
CN1306-11	49.3208	-67.6371	North-Shore	Bulk	0.9760	0.0218	0.0022	533.9129	28.44	11.15	52.99	64.14	1.92	0.01	0.01	0.1	3.72	0.66	315	0.200	23.728
CN1306-12	49.4183	-67.3060	North-Shore	Bulk	0.9465	0.0489	0.0046	441.4969	35.28	10.83	46.38	57.21	2.18	0.18	0.31	0.1	3.72	0.3	367	0.177	21.821
CN1306-13	49.7584	-67.1771	North-Shore	Bulk	0.9837	0.0144	0.0019	706.7019	29.14	13.62	50.66	64.28	0.96	0.01	0.01	0.06	4.39	0.3	111	0.196	23.044
CN1306-14	50.0316	-66.8752	North-Shore	Bulk	1.0000	0.0000	0.0000	701.5333	39.87	11.87	38.07	49.94	1.96	1.39	0.61	0.42	5.14	0.01	249	0.319	31.600
CN1306-15	50.1475	-66.5874	North-Shore	Bulk	0.9685	0.0286	0.0028	341.1445	29.36	11.73	47.03	58.76	3.25	0.26	0.12	0.4	6.52	0.61	550	0.301	32.215
CN1306-16	50.1940	-66.0918	North-Shore	Bulk	0.9947	0.0041	0.0012	417.6643	16.22	6.7	33.19	39.89	7.07	1.86	15.72	11.71	5.99	0.46	1560	11.555	12.215
CN1306-17	50.2654	-66.0349	North-Shore	Bulk	0.9910	0.0071	0.0019	437.2566	24.54	9.75	49.91	59.66	3.58	1.08	0.48	0.56	7.35	1.33	2576	0.678	27.475
CN1306-18	50.2704	-64.9193	North-Shore	Bulk	0.9831	0.0153	0.0016	762.2209	15.22	6.77	64	70.77	2.72	1.66	0.25	0.15	6.67	1.37	589	0.642	16.664
CN1306-19	50.2927	-64.3263	North-Shore	Bulk	0.6732	0.3087	0.0181	76.8213	21.21	10.18	60.43	70.61	1.89	0.01	0.26	0.17	3.96	1.07	487	0.534	19.134
CN1306-20	50.3029	-64.0004	North-Shore	Bulk	0.9194	0.0766	0.0040	364.6322	16.47	7.07	64.82	71.89	1.78	0.08	0.8	0.42	6.56	1	932	0.611	24.459
CN1306-21	50.3074	-63.7874	North-Shore	Bulk	0.9170	0.0757	0.0073	210.3808	31.75	11.73	50.57	62.3	0.81	0.57	0.34	0.36	3.05	0.17	550	0.237	22.304
CN1306-22	50.2886	-62.8916	North-Shore	Bulk	0.9752	0.0222	0.0026	633.9852	44.02	7.5	33.92	41.42	6.7	0.12	0.48	0.3	3.23	2.65	689	0.315	22.870
CN1306-23	50.2875	-62.8076	North-Shore	Bulk	0.9776	0.0197	0.0027	836.9989	39.67	11.01	31.59	42.6	1.76	0.54	0.22	0.33	7.64	1.92	356	0.807	36.357
CN1306-24	50.2280	-62.1105	North-Shore	Bulk	0.9774	0.0193	0.0033	275.6544	33.73	16.18	42.69	58.87	1.56	1.19	0.84	0.36	2.57	0.16	1157	0.394	27.820
CN1306-25	50.1875	-61.8223	North-Shore	Bulk	1.0000	0.0000	0.0000	316.1305	36.08	19.6	39.2	58.8	1.13	0.77	0.16	0.13	1.98	0.1	190	0.121	10.479
CN1306-26	50.1287	-61.8055	North-Shore	Bulk	0.9850	0.0131	0.0019	551.7998	32.55	16.72	42.4	59.12	1.35	1.38	0.7	0.44	2.72	0.57	1135	0.484	22.487
CN1306-27	50.1532	-61.6291	North-Shore	Bulk	0.8702	0.1198	0.0099	223.8835	38.04	20.9	36.51	57.41	0.6	0.58	0.26	0.27	2.12	0.12	773	0.328	21.857
CN1306-28	50.2770	-64.7808	North-Shore	Bulk	NaN	NaN	NaN	NaN	16.45	7.44	62.7	70.14	4.42	0.01	0.29	0.31	5.49	1.7	416	0.493	24.240
CN1306-29	50.3170	-65.2425	North-Shore	Bulk	0.9825	0.0150	0.0024	576.9644	22.48	8.77	47.06	55.83	5.39	1.67	4.14	0.64	6.44	1.46	4819	1.582	30.420
CN1306-01	48.0948	-69.2149	South-Shore	Bulk	0.9527	0.0431	0.0042	723.5378	53.31	2.32	14.18	16.5	0.01	0.01	0.18	0.24	18.82	8.73	31	0.036	8.483
CN1306-02	48.1318	-69.1847	South-Shore	Bulk	0.1404	0.7914	0.0681	16.4801	39.61	8.37	26.38	34.75	0.47	1.12	0.34	0.03	17.58	5.05	119	0.216	10.391
CN1306-30	48.8206	-67.5353	South-Shore	Bulk	0.9811	0.0155	0.0033	897.8175	56.1	0.74	11.7	12.44	0.49	0.01	0.34	0.2	15.9	12	88	0.054	20.284
CN1306-31	48.8531	-67.5290	South-Shore	Bulk	0.9917	0.0064	0.0019	547.4478	59.31	2.53	16	18.53	0.19	0.01	0.08	0.04	10.42	8.19	51	0.031	9.634
CS1309-01	48.6254	-68.1297	South-Shore	Bulk	0.9341	0.0610	0.0049	724.0785	47.48	3.04	14.94	17.98	0.01	0.01	0.18	0.05	22.11	7.41	23	0.039	9.361
CS1309-02	49.0983	-66.6769	South-Shore	Bulk	0.9068	0.0876	0.0056	353.2324	38.84	1.98	16.13	18.11	2.21	1.05	0.62	0.1	21.3	15.79	224	0.132	20.733
CS1309-03	49.1224	-66.5004	South-Shore	Bulk	0.9318	0.0641	0.0041	490.3027	39.54	2.84	15.28	18.12	0.45	0.82	0.18	0.2	26.01	12.42	119	0.114	19.255
CS1309-04	49.2237	-65.7968	South-Shore	Bulk	0.9608	0.0357	0.0035	396.0585	40.17	1.45	13.76	15.21	0.01	0.01	0.06	0.01	29.24	13.08	34	0.026	5.806
CS1309-05	49.2296	-65.7360	South-Shore	Bulk	0.9032	0.0897	0.0071	478.7751	44.56	2.51	15.2	17.71	0.01	0.53	0.19	0.03	25.18	9.94	74	0.068	13.501
CS1309-06	49.2388	-65.3114	South-Shore	Bulk	0.9450	0.0498	0.0052	583.4785	52.13	4.75	16.61	21.36	0.01	0.34	0.15	0.01	17.44	6.92	61	0.049	9.851

CS1309-07	49.2250	-65.1281	South-Shore	Bulk	0.9885	0.0091	0.0024	515.1955	57.95	3.05	12.94	15.99	0.01	0.01	0.18	0.01	19.57	5.06	9	0.013	2.194
CS1309-08	48.9956	-64.3975	South-Shore	Bulk	0.9643	0.0311	0.0047	686.9548	49.53	1.67	13.13	14.8	0.01	0.01	0.47	0.01	24.91	8.17	11	0.008	1.673
CS1309-09	48.9375	-64.3091	South-Shore	Bulk	0.2642	0.6953	0.0405	26.3179	51.68	1.74	14.54	16.28	0.01	0.23	0.32	0.01	23.28	6.32	5	0.014	1.322
CS1309-10	49.2523	-65.5444	South-Shore	Bulk	1.0000	0.0000	0.0000	681.6216	42.44	1.85	15.24	17.09	0.01	0.67	0.06	0.01	27.75	10.06	16	0.028	4.115
CS1309-11	49.2069	-66.1697	South-Shore	Bulk	1.0000	0.0000	0.0000	1035.8120	46.92	2.09	14.24	16.33	0.01	0.01	0.05	0.01	24.75	10.1	14	0.013	1.182
CS1309-12	48.7556	-67.7951	South-Shore	Bulk	1.0000	0.0000	0.0000	807.1183	56.6	2.6	14.77	17.37	0.01	0.01	0.29	0.44	16.9	7.04	22	0.041	9.077
CS1406-00	NaN	NaN	South-Shore	Bulk	NaN	NaN	NaN	NaN	52.86	3.06	20.9	23.9	0.0	0.0	0.2	0.0	14.7	6.8	NaN	NaN	NaN
CS1406-01	NaN	NaN	South-Shore	Bulk	NaN	NaN	NaN	NaN	43.35	7.46	29.1	36.6	0.5	0.0	0.0	0.1	13.3	5.1	NaN	NaN	NaN
CS1406-02	NaN	NaN	South-Shore	Bulk	NaN	NaN	NaN	NaN	49.72	6.55	34.5	41.1	0.4	0.0	0.0	0.1	5.6	2.1	NaN	NaN	NaN
CS1406-03	NaN	NaN	South-Shore	Bulk	NaN	NaN	NaN	NaN	48.66	7.82	32.7	40.5	0.4	0.0	0.0	0.1	7.2	2.5	NaN	NaN	NaN
COR0307-47	48.8124	-68.6729	Laurentian Channel	Bulk	0.0000	0.8994	0.1006	8.3046	24.24	14.14	40.06	54.2	1.54	0.84	0.64	0.16	15.58	2.01	NaN	NaN	NaN
COR0503-05	48.8648	-68.6530	Laurentian Channel	Bulk	0.3097	0.6318	0.0585	23.2266	20.88	15.08	30.14	45.22	0.74	0.31	0.43	0.22	24.69	6.5	426	0.380	23.081
COR0503-14	49.6801	-65.1503	Laurentian Channel	Bulk	0.0663	0.8584	0.0753	11.1385	23.52	14.1	27.25	41.35	0.73	0.87	0.39	0.21	25.42	6.41	49	0.451	18.391
COR0503-39	48.8603	-68.5310	Laurentian Channel	Bulk	0.0656	0.8051	0.1293	8.5902	25.06	12.67	34.49	47.16	1.27	0.43	0.47	0.28	20.46	4.06	82	0.353	18.757
COR0503-40	48.8072	-68.7205	Laurentian Channel	Bulk	0.1177	0.7623	0.1200	12.2414	24.58	12.96	38.23	51.19	1.28	1.21	0.56	0.13	18.28	2.23	156	0.430	21.301
COR0602-43	49.1183	-67.2783	Laurentian Channel	Bulk	0.0152	0.8791	0.1058	7.8040	22.97	15.14	31.53	46.67	0.93	0.53	0.56	0.19	23.15	3.93	64	0.495	11.812
COR0703-06	49.0493	-67.8621	Laurentian Channel	Bulk	0.0092	0.8886	0.1022	8.0762	25.6	13.42	34.18	47.6	0.99	0.01	0.36	0.14	20.28	4.5	61	0.392	20.657
COR0703-08	49.0717	-67.9190	Laurentian Channel	Bulk	0.3817	0.5608	0.0575	31.4384	32.96	12.14	43.42	55.56	1.68	0.74	0.27	0.19	7.56	0.68	224	0.382	22.414
COR0703-12	48.8097	-68.6401	Laurentian Channel	Bulk	0.0019	0.8809	0.1172	7.4365	24.45	13.51	34.03	47.54	1.18	0.54	0.65	0.21	20.49	4.07	56	0.308	20.213
COR1002-28	48.9180	-67.5946	Laurentian Channel	Bulk	NaN	NaN	NaN	NaN	27.25	13.11	30.53	43.64	0.86	0.57	0.56	0.19	20.95	4.97	80	0.383	20.764
COR1004-23	48.7032	-68.6335	Laurentian Channel	Bulk	0.0000	0.8930	0.1070	7.3724	22.67	13.73	31.05	44.78	0.74	0.95	0.42	0.12	23.43	5.82	46	0.353	20.514
COR1203-14	48.4736	-69.0417	Laurentian Channel	Bulk	NaN	NaN	NaN	NaN	25.83	15.15	31.54	46.69	0.82	0.63	0.59	0.23	19.74	4.46	66	0.292	18.599
COR1203-17	49.1925	-67.8534	Laurentian Channel	Bulk	0.0686	0.8292	0.1022	9.4803	24.66	14.88	37.1	51.98	1.41	1.01	0.33	0.15	16.91	2.9	136	0.493	21.345
COR1203-22	49.2063	-67.9958	Laurentian Channel	Bulk	0.0907	0.8465	0.0628	12.9136	24.54	14.85	36.62	51.47	1.51	0.44	0.59	0.32	18.04	2.27	98	0.329	18.642
COR1203-27	49.2638	-67.3859	Laurentian Channel	Bulk	0.0596	0.8754	0.0649	12.7015	23.47	15.22	34.84	50.06	1.23	1.48	0.5	0.3	20.14	2.23	134	0.505	18.405
MS11-EM09	48.3341	-69.2573	Laurentian Channel	Bulk	0.0000	0.8038	0.1962	4.9301	24.66	12.56	33.46	46.02	1.12	1.23	0.5	0.18	21.4	4.31	NaN	NaN	NaN
MS11-EM10	NaN	NaN	Laurentian Channel	Bulk	NaN	NaN	NaN	NaN	25.6	14.04	32.59	46.63	1	0.73	0.53	0.4	20.32	4.09	NaN	NaN	NaN
MS11-EM15		NaN	Laurentian Channel	Bulk	0.0000	0.8038	0.1962	4.9702	26.17	12.91	31.67	44.58	0.92	0.64	0.59	0.03	20.4	5.62	NaN	NaN	NaN
MS11-EM22	48.8886	-68.3631	Laurentian Channel	Bulk	0.0000	0.7983	0.2017	4.7251	24.83	14.77	32.92	47.69	0.81	0.28	0.27	0.09	20.43	4.6	NaN	NaN	NaN
MS12-12	48.7620	-68.7240	Laurentian Channel	Bulk	0.0838	0.8078	0.1084	10.1168	27.11	15.19	39.53	54.72	1.66	0.65	0.69	0.31	12.67	1.56	210	0.313	19.585
MS12-13	48.7330	-68.7410	Laurentian Channel	Bulk	0.2952	0.6209	0.0838	18.1567	30.9	12.83	42.71	55.54	1.23	1.06	0.52	0.04	8.81	1.19	255	0.265	18.851
MS12-EM14	48.6870	-68.6910	Laurentian Channel	Bulk	0.0061	0.8806	0.1133	7.3113	22.62	15.09	29.79	44.88	0.95	1.33	0.31	0.01	22.98	5.9	39	0.249	13.499
MS13-EM4	48.3840	-69.1950	Laurentian Channel	Bulk	0.0000	0.7997	0.2003	5.9967	27.37	14.71	30.31	45.02	0.92	0.58	0.5	0.24	19.69	4.57	NaN	NaN	NaN
MS13-EM6	48.7000	-68.6570	Laurentian Channel	Bulk	0.0000	0.7974	0.2026	5.5578	23.34	14.22	31.8	46.02	0.86	0.01	0.41	0.33	23.3	4.5	NaN	NaN	NaN
COR0307-49	48.9936	-68.1971	North-Margin	Bulk	NaN	NaN	NaN	NaN	27.09	13.34	40.28	53.62	1.59	0.8	0.43	0.28	13.58	1.8	NaN	NaN	NaN
COR0307-52	48.8785	-68.7172	North-Margin	Bulk	0.3424	0.6198	0.0378	30.3431	25.65	12.64	47.46	60.1	2.69	1.88	0.62	0.19	7.79	0.52	NaN	NaN	NaN
COR0503-02	48.8454	-68.7344	North-Margin	Bulk	NaN	NaN	NaN	NaN	24.83	13.13	45.34	58.47	2.13	1.2	0.67	0.16	11.04	0.87	290	0.424	17.384
COR0503-04	48.8595	-68.7225	North-Margin	Bulk	0.2876	0.6252	0.0872	20.2130	24.95	13.23	49.25	62.48	2.55	2.13	0.52	0.01	6.43	0.5	621	0.489	20.101
COR0503-08	50.0452	-66.3782	North-Margin	Bulk	0.0762	0.8512	0.0726	12.0235	27.44	11.65	48.59	60.24	2.2	0.01	0.33	0.21	8.23	1.02	395	0.414	17.627
COR0503-11	50.0422	-66.3460	North-Margin	Bulk	0.3277	0.6315	0.0408	27.0176	27.09	11.64	48.8	60.44	2.91	0.18	0.44	0.4	7.5	0.52	734	0.510	19.756

COR0503-12	50.0931	-66.3284	North-Margin	Bulk	0.4364	0.5205	0.0431	38.2687	27.62	12.6	46.24	58.84	2.78	0.54	0.44	0.36	7.89	0.74	536	0.413	22.128
COR0503-13	50.2251	-63.9662	North-Margin	Bulk	0.5691	0.4057	0.0251	58.4687	24.81	11.15	54.57	65.72	2.2	0.17	0.31	0.26	5.19	0.33	551	0.411	24.712
COR0602-09	48.8267	-68.7733	North-Margin	Bulk	NaN	NaN	NaN	NaN	25.37	12.12	47.66	59.78	2.34	0.66	0.47	0.23	10.06	0.64	420	0.496	23.306
COR0602-45	49.4233	-66.3217	North-Margin	Bulk	0.0293	0.8920	0.0787	10.0286	24.59	13.22	47.63	60.85	2.26	1.42	0.55	0.18	8.62	0.78	45	0.501	9.197
COR0602-49	50.0417	-66.3450	North-Margin	Bulk	0.3265	0.6452	0.0282	32.9152	25.31	13.13	43.48	56.61	3.03	1.52	0.67	0.45	10.97	1.02	NaN	NaN	NaN
COR0602-51	50.0433	-66.3917	North-Margin	Bulk	0.3303	0.6407	0.0290	32.6412	25.79	13.11	43.15	56.26	2.7	1.42	0.54	0.32	11.26	1.01	NaN	NaN	NaN
COR0602-55	49.9833	-66.6350	North-Margin	Bulk	0.0952	0.8493	0.0556	15.0631	23.66	11.7	46	57.7	2.25	0.92	0.47	0.51	12.7	0.99	423	0.656	25.059
COR0602-57	50.1850	-66.4733	North-Margin	Bulk	0.0444	0.9011	0.0545	15.1123	21.44	14.48	41.07	55.55	2.85	1.13	0.57	1.44	15.44	0.96	NaN	NaN	NaN
COR0602-58	50.1450	-66.3267	North-Margin	Bulk	0.0974	0.8344	0.0682	13.7600	24.72	13.76	41.14	54.9	2.23	1.16	0.48	0.9	14.14	0.83	355	0.538	21.235
COR0602-61	50.1450	-66.3267	North-Margin	Bulk	0.3427	0.6348	0.0225	36.3806	25.33	13.11	44.82	57.93	2.65	0.16	0.53	0.5	11.61	0.46	NaN	NaN	NaN
COR0602-63	50.0900	-66.2667	North-Margin	Bulk	0.2761	0.6813	0.0426	26.5161	29.06	12.72	45.46	58.18	1.55	0.44	0.79	0.28	7.89	0.9	NaN	NaN	NaN
COR0602-64	50.0640	-65.9980	North-Margin	Bulk	0.6544	0.3214	0.0242	122.8742	29.52	13.36	45.75	59.11	1.16	0.01	0.2	0.23	8.46	0.86	330	0.380	20.130
COR0703-10	48.8615	-68.6945	North-Margin	Bulk	0.3411	0.5814	0.0775	24.1164	28.07	12.26	49.09	61.35	2.11	0.59	0.48	0.11	6.28	0.53	660	0.468	26.395
COR0703-14	48.8517	-68.6207	North-Margin	Bulk	0.2671	0.6630	0.0698	18.5991	27.82	13.54	44.5	58.04	2.07	0.97	0.61	0.08	9.1	0.69	388	0.371	24.472
COR1002-13	50.1751	-66.3360	North-Margin	Bulk	0.5727	0.4025	0.0249	52.9809	26.73	14.27	44.22	58.49	2.31	0.35	0.46	0.43	10.02	0.61	642	0.398	18.102
COR1002-15	50.1724	-66.3312	North-Margin	Bulk	0.4275	0.5389	0.0336	35.7840	25.08	13.41	45.05	58.46	3.32	0.15	0.59	0.42	10.64	0.57	580	0.456	63.698
COR1002-16	50.1720	-66.3427	North-Margin	Bulk	0.3963	0.5715	0.0322	34.1628	25.26	13.16	43.87	57.03	2.53	0.33	0.41	0.73	12.34	0.75	547	0.431	17.706
COR1002-17	50.1786	-66.3312	North-Margin	Bulk	0.3873	0.5779	0.0348	32.3560	25.12	13.62	42.7	56.32	2.72	0.01	0.5	0.59	13.04	0.89	467	0.322	21.270
COR1002-18	50.1798	-66.3390	North-Margin	Bulk	0.6257	0.3512	0.0231	57.6897	23.7	12.29	48.44	60.73	2.59	0.81	0.63	0.64	9.64	0.73	693	0.390	19.836
COR1002-19	50.1856	-66.3408	North-Margin	Bulk	0.6520	0.3280	0.0199	69.2562	24.69	11.51	44.19	55.7	2.77	0.4	0.47	0.92	13.37	1.12	633	0.358	23.771
COR1002-20	50.1851	-66.3426	North-Margin	Bulk	0.6362	0.3412	0.0225	58.1226	26.16	14.56	40.58	55.14	2.58	1.31	0.48	0.74	12.08	0.98	581	0.349	25.875
COR1002-21	50.1760	-66.3443	North-Margin	Bulk	0.2926	0.6576	0.0497	22.0794	23.99	12.79	41.64	54.43	2.94	0.31	0.63	1.16	14.72	1.01	644	0.427	23.014
COR1002-27	49.2897	-67.3607	North-Margin	Bulk	0.2943	0.6503	0.0553	21.3352	25.89	14.82	41.45	56.27	1.65	0.79	0.62	0.35	13.22	0.7	271	0.408	24.352
COR1203-01	48.1483	-69.6019	North-Margin	Bulk	0.9617	0.0309	0.0075	482.5182	35.11	12.4	43.19	55.59	1.1	0.6	0.56	0.02	5.43	0.94	666	0.413	25.441
COR1203-02	48.1529	-69.5808	North-Margin	Bulk	0.6610	0.2983	0.0407	94.7188	29.43	12.56	50.3	62.86	1.25	0.19	0.1	0.29	4.18	0.8	592	0.386	26.617
COR1203-03	48.1580	-69.5910	North-Margin	Bulk	0.9446	0.0428	0.0126	336.7483	34.11	12.36	44.83	57.19	1.17	0.45	0.67	0.15	5.3	0.52	624	0.277	26.753
COR1203-05	48.1871	-69.5922	North-Margin	Bulk	0.6023	0.3416	0.0561	50.6344	32.79	12.67	44.62	57.29	1.36	0.52	0.65	0.13	5.94	0.72	741	0.355	28.191
COR1203-06	48.1907	-69.5820	North-Margin	Bulk	0.5715	0.3740	0.0546	70.1694	34.61	12.57	44.79	57.36	0.98	0.21	0.51	0.07	5.36	0.56	492	0.326	19.676
COR1203-08	48.2007	-69.5730	North-Margin	Bulk	0.8043	0.1709	0.0247	249.2824	37.02	12.81	40.9	53.71	0.9	0.71	0.76	0.19	5.73	0.54	644	0.371	21.947
COR1203-09	48.1807	-69.5690	North-Margin	Bulk	0.4146	0.5086	0.0768	25.4595	30.08	13.6	44.17	57.77	1.52	0.49	0.53	0.17	7.72	0.71	453	0.379	23.832
COR1203-19	49.2594	-67.5265	North-Margin	Bulk	0.3464	0.6010	0.0526	24.0913	29.27	13.91	43.25	57.16	1.89	0.51	0.51	0.17	9.16	0.24	410	0.346	22.618
COR1203-20	49.2520	-67.5686	North-Margin	Bulk	0.4980	0.4660	0.0359	37.6015	26.64	14.88	46.73	61.61	2.58	1.46	0.4	0.11	6.23	0.32	458	0.313	22.651
COR1203-21	49.2341	-67.6182	North-Margin	Bulk	0.0739	0.8710	0.0551	14.8311	24.21	14.35	42.12	56.47	1.93	0.28	0.35	0.37	14.27	1.29	181	0.341	20.644
COR1203-25	49.2870	-67.4018	North-Margin	Bulk	0.5869	0.3734	0.0397	45.1635	28.25	14.93	43.37	58.3	1.82	1.23	0.52	0.26	9.25	0.04	401	0.286	18.430
COR1203-26	49.2956	-67.3822	North-Margin	Bulk	0.6686	0.3077	0.0237	59.8557	28.56	13.84	44.54	58.38	1.79	0.86	0.13	0.19	9.15	0.41	503	0.220	17.679
MS11-EM13	NaN	NaN	North-Margin	Bulk	0.0000	0.7727	0.2273	4.5827	26.76	14.55	41.7	56.25	1.34	0.52	0.56	0.15	11.91	2.07	NaN	NaN	NaN
MS11-EM17	NaN	NaN	North-Margin	Bulk	0.0000	0.7716	0.2284	4.5419	33.31	10.55	44.73	55.28	1.93	0.36	0.46	0.11	6.77	1.01	NaN	NaN	NaN
MS11-EM19	48.9571	-68.5410	North-Margin	Bulk	0.0000	0.8288	0.1712	6.1903	24.23	11.2	44.33	55.53	2.28	0.07	0.44	0.18	15.19	1.31	NaN	NaN	NaN
MS11-EM20	48.9087	-68.4936	North-Margin	Bulk	0.0000	0.8502	0.1498	6.0873	31.32	9.09	46.01	55.1	1.98	1.56	0.26	0.35	8.25	0.8	NaN	NaN	NaN
MS12-10	48.8250	-68.8040	North-Margin	Bulk	0.9478	0.0449	0.0073	434.7829	32.29	11.75	49.19	60.94	1.87	1.43	0.36	0.2	2.32	0.24	621	0.274	20.067

MS12-11	48.8220	-68.7990	North-Margin	Bulk	0.7744	0.2009	0.0247	200.6022	32.35	12.68	47.63	60.31	1.53	0.58	0.37	0.1	3.6	0.6	497	0.254	20.549
COR0602-38	48.3650	-69.0650	South-Margin	Bulk	0.2250	0.6922	0.0828	15.6604	31.44	13.02	36.18	49.2	1.3	0.66	0.64	0.23	12.87	2.89	313	0.407	15.786
MS11-EM23	48.6909	-68.2853	South-Margin	Bulk	0.0000	0.8445	0.1555	5.9663	29.12	13.27	33.61	46.88	1.19	0.7	0.52	0	16.75	4.03	NaN	NaN	NaN
MS11-EM24	48.6649	-68.2776	South-Margin	Bulk	0.0000	0.7966	0.2034	5.1081	30.48	12.4	35.93	48.33	1.14	0	0.47	0.18	15.31	3.1	NaN	NaN	NaN
MS11-EM25	48.6559	-68.2753	South-Margin	Bulk	0.0000	0.8219	0.1781	5.6965	31.06	12.53	37.5	50.03	1.18	0.19	0.42	0.05	13.49	2.68	NaN	NaN	NaN
MS12-EM45	48.3714	-68.9179	South-Margin	Bulk	0.6535	0.2980	0.0485	83.7494	40.19	10.98	35.82	46.8	1.16	0.58	0.56	0.1	8.24	1.3	552	0.238	21.702
MS13-EM10	48.5420	68.6230	South-Margin	Bulk	0.3614	0.5298	0.1059	31.8697	33.87	12.28	40.53	52.81	1.71	0.15	0.47	0.11	8.29	1.66	NaN	NaN	NaN
MS13-EM8	48.5930	-68.5560	South-Margin	Bulk	0.0718	0.7828	0.1454	9.5741	31.63	12.3	32.83	45.13	0.77	0.01	0.86	0.01	16.66	3.86	NaN	NaN	NaN
MS13-EM9	48.5800	-68.5560	South-Margin	Bulk	0.1598	0.6774	0.1628	12.3569	31.78	14.3	35.37	49.67	1.17	0.1	0.83	0.39	12.6	2.63	NaN	NaN	NaN